Since January 2020 Elsevier has created a COVID-19 resource centre with free information in English and Mandarin on the novel coronavirus COVID-19. The COVID-19 resource centre is hosted on Elsevier Connect, the company's public news and information website.

Biosensors and Bioelectronics 166 (2020) 112471

Contents lists available at ScienceDirect

Biosensors and Bioelectronics

journal homepage: http://www.elsevier.com/locate/bios

Graphene biosensors for bacterial and viral pathogens

Zixin Jiang [a], Bo Feng [a,**], Jin Xu [a], Taiping Qing [a,***], Peng Zhang [a], Zhihe Qing [b,*]

[a] College of Environment and Resources, Xiangtan University, Xiangtan, 411105, Hunan Province, China
[b] Hunan Provincial Key Laboratory of Cytochemistry, School of Chemistry and Food Engineering, Changsha University of Science and Technology, Changsha, 410114, Hunan Province, China

ARTICLE INFO

Keywords:
Graphene
Bio-functionalization
Biosensing
Pathogens

ABSTRACT:

The infection and spread of pathogens (e.g., COVID-19) pose an enormous threat to the safety of human beings and animals all over the world. The rapid and accurate monitoring and determination of pathogens are of great significance to clinical diagnosis, food safety and environmental evaluation. In recent years, with the evolution of nanotechnology, nano-sized graphene and graphene derivatives have been frequently introduced into the construction of biosensors due to their unique physicochemical properties and biocompatibility. The combination of biomolecules with specific recognition capabilities and graphene materials provides a promising strategy to construct more stable and sensitive biosensors for the detection of pathogens. This review tracks the development of graphene biosensors for the detection of bacterial and viral pathogens, mainly including the preparation of graphene biosensors and their working mechanism. The challenges involved in this field have been discussed, and the perspective for further development has been put forward, aiming to promote the development of pathogens sensing and the contribution to epidemic prevention.

1. Introduction

Pathogens refer to the microorganisms (including bacteria, viruses, fungi, etc.) and parasites that can cause infections of organisms, among which bacteria and viruses are the most common and harmful. They infect humans, plants and animals in a variety of ways – through food, air and water, and are estimated to be responsible for more than 15 million deaths worldwide each year (Dye, 2014). For a long time, common bacterial infections and contagious viruses have posed enormous challenges to people around the world. For example, the COVID-19 virus, which the world is now doing its utmost to combat, has not only caused millions of infections and hundreds of thousands of deaths, but also had a massive impact on the world economy. On the one hand, this event has struck a bell for us to respect nature and protect the environment. And on the other hand, it also reflects the importance of timely and accurate detection of pathogens for rapid isolation and treatment.

Traditional pathogen analysis techniques such as polymerase chain reaction (PCR) (Klein, 2002) and enzyme-linked immunosorbent assay (ELISA) (Law et al., 2015) are highly sensitive and durable. Whereas, they also have the drawbacks of laborious testing process, time-consuming pretreatment, and requirement of professional equipment and personnel. As a result, it is necessary to develop alternative analytical techniques for rapid, sensitive and real-time continuous monitoring of pathogens (Choi, 2020). Biosensor, as the name implies, is a type of analytical device that integrates the biological recognition with physical-chemical detectors for analytes detection. Thanks to their superior performance such as high selectivity and sensitivity, low cost, high-efficiency, miniaturization, etc., to date, biosensors have been widely developed and applied in food safety, environmental monitoring and clinical diagnosis.

The rapid advance of nanoscience and nanotechnology makes it possible to design nanomaterials-assisted biosensors with improved detection performance for pathogenic bacteria and virus (Li et al., 2019b; Qing et al., 2020a; Qing et al., 2020c; Sanvicens et al., 2009). Because the small size, unique properties (e.g., fluorescence quenching and electroconductivity) and good biocompatibility of graphene are just in keeping with the high-efficiency and diversity required for biosensors, graphene-based biosensors have been intensely developed in the past decades (Zhu et al., 2017). Compared to other nanomaterials sensors,

* Corresponding author.
** Corresponding author.
*** Corresponding author.
E-mail addresses: fengbo@xtu.edu.cn (B. Feng), taiping_qing@163.com (T. Qing), qingzhihe@hnu.edu.cn (Z. Qing).

https://doi.org/10.1016/j.bios.2020.112471
Received 18 June 2020; Received in revised form 14 July 2020; Accepted 21 July 2020
Available online 25 July 2020

graphene-based biosensors embody various unique advantages. For example, the unique 2D structure and single-atom thickness of graphene sheets enable each carbon atom to interact with the analyte directly, thereby allowing graphene-based biosensors to be highly sensitive to any tiny changes in the surrounding environmental conditions (Justino et al., 2017). And due to their large surface with aromatic structure and rich active sites, graphene exhibits a high loading capacity for a variety of molecules, which broadens the detection category and range of graphene biosensors (Zhang et al., 2017c). Besides, in contrast to carbon nanotubes (CNTs) or other 2D nanomaterials, there are no metal impurities in graphene that interfere with electrochemistry or other signals (Pumera et al., 2010), so that the graphene sensors can be integrated with a variety of signal transduction technologies, promoting their diverse development.

Here, inspired by the importance of pathogens determination and the advantage of graphene biosensors, we focus on the detection of pathogens based on graphene biosensors (Scheme 1). The physicochemical and biological properties of graphene, bio-functionalization, biosensing mechanism and challenges were reviewed and discussed.

2. Graphene

Graphene, a one-atom-thick two-dimensional carbon nanomaterial with hexagonal honeycomb lattice, was isolated from graphite for the first time in 2004 (Allen et al., 2010). Since then, graphene and its derivatives have attracted extensive attention owing to the unique optical properties, superb conductivity, excellent mechanical strength, and vast specific surface areas (Hu et al., 2017; Hu et al., 2019; Justino et al., 2017; Song et al., 2016). They are considered to be a revolutionary material in the future and have important application prospects in materials science, energy, biosensing, biomedicine, and drug delivery. In this part, we will briefly summarize the preparation methods of graphene and their relevant properties (including physicochemical properties, biocompatibility, antibacterial and antiviral effects).

2.1. Preparation of graphene

In the past dozen years, various methods for graphene preparation have been reported, such as micromechanical exfoliation, oxidation-reduction method, epitaxial growth, chemical vapor deposition (CVD) and so on (Sanni et al., 2019). One of the most common is micromechanical exfoliation, which utilizes the friction and relative motion between graphite and objects to produce thin layer of graphene (Huang et al., 2015b). This method has low cost and simple operation, and is capable of obtaining graphene with an intact crystal structure. However, it is only suitable for basic scientific researches and is difficult to achieve large-scale production and application owing to the uncontrollability of graphene's size, shape and layers (Wei and Liu, 2010).

The oxidation-reduction method is also considered to be an excellent method for preparing graphene, which first oxidizes natural graphite with strong oxidizing agents to generate graphene oxide (GO), and then reduces them chemically, thermally, etc. This strategy is able to produce graphene on a massive scale, and can also prepare GO and reduced GO (rGO) with rich surface functional groups. The synthesis of graphene by CVD is mainly based on carbon organic gases such as methane and ethanol. Although CVD is currently expensive and imperfect, it is believed to be the most promising method for industrialized production of graphene (Reina et al., 2009). High-quality graphene can also be obtained by SiC epitaxial growth, while the strict high vacuum and temperature control are required (Akcöltekin et al., 2009). In addition, more and more novel and effective methods for preparing graphene are emerging as research continues (Sha et al., 2017; Voiry et al., 2016; Wang et al., 2017).

2.2. Properties of graphene

As a result of the unique two-dimensional structure, graphene materials exhibit excellent properties in all aspects. Among them, the most remarkable is their superior electronic properties. It was found that the electron mobility in graphene could be as high as 10,000–50,000 cm^2 V^{-1} s^{-1} at room temperature, and the intrinsic mobility limit also exceeds 200,000 cm^2 V^{-1} s^{-1} (Bolotin et al., 2008; Sreeprasad and Berry, 2013). Notably, unlike most other materials, the electron mobility of graphene is less affected by temperature changes. The electrical conductivity of graphene could be up to 10^8 mS cm^{-1}, which is usually related to the preparation or treatment methods and the morphology of

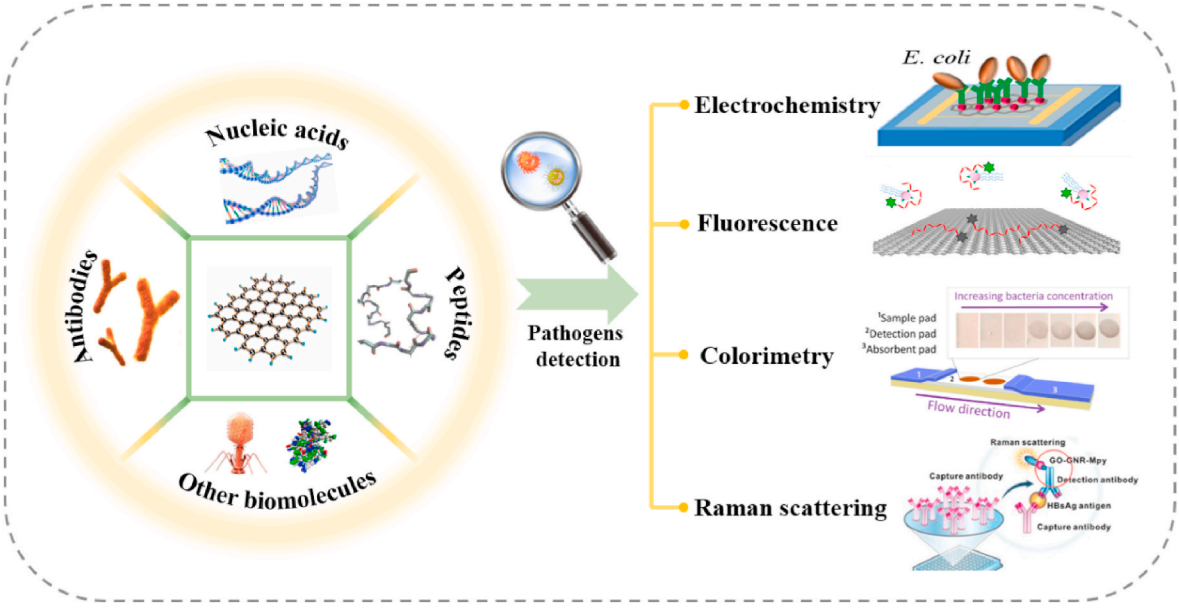

Scheme 1. Biofunctionalized graphene biosensors for the detection of bacterial and viral pathogens. Electrochemical graphene biosensor. (Reproduced with permission from Ref. (Thakur et al., 2018). Copyright 2018, Elsevier). Fluorescent graphene biosensor. (Reproduced with permission from Ref. (Niu et al., 2018a). Copyright 2018, American Chemical Society). Colorimetric graphene biosensor. (Reproduced with permission from Ref. (Shirshahi et al., 2019). Copyright 2019, Elsevier). Surface-enhanced Raman scattering-based graphene biosensor. (Reproduced with permission from Ref. (Liu et al., 2018c). Copyright 2018, Springer).

the graphene particles (Bahadır and Sezgintürk, 2016). Graphene exhibits a half-integer Quantum Hall Effect (QHE) due to the similar charge carrier behavior to semi-metals (commonly known as massless Dirac Fermions) (Tiwari et al., 2016). Thus, the distinct QHE could be observed in graphene and presents a peculiar relationship between charge, thickness and charge carrier velocity. In addition, graphene has a lamellar structure with large theoretical specific surface area of 2630 m^2/g (Stoller et al., 2008). And the abundant carboxyl, hydroxyl and epoxy groups on the surface also provide a great convenience for the modification of other molecules or the occurrence of surface reactions.

In the meantime, graphene also possesses outstanding optical properties. For example, graphene has an extremely high quenching efficiency for the fluorescence of various organic dyes and quantum dots, and the quenching distance is up to 30 nm (Swathi and Sebastian, 2009). This optical phenomenon mainly derives from the non-radiative dipole-dipole interaction or fluorescence resonance energy transfer (FRET) between graphene and fluorescent substances (Anju and Renuka, 2019). FRET, a non-optical physical process, is based on the non-radiation energy transfer between the donor and the acceptor at an appropriate distance, in which the donor's emission spectrum overlaps the acceptor's absorption spectrum to some extent. Theoretical and experimental studies have indicated that both energy transfer and electron transfer can induce the quenching of fluorophores on graphene, while the quenched fluorescence could be recovered gradually with the increase of their distance, which offers a new idea for the development of fluorescent sensors (Wang et al., 2016; Zhu et al., 2015). Except as a powerful fluorescence quenching agent, graphene also has a tunable photoluminescence property that arises from the small sp^2 graphite clusters embedded in the sp^3 matrix (Liu et al., 2011). Moreover, graphene has the ability to assist in improving the performance of some optical sensors. It has been reported that the surface-enhanced Raman scattering (SERS) and surface plasmon resonance (SPR) signals could be greatly amplified due to the charge transfer between graphene and probe molecules (Ling et al., 2010; Patil et al., 2019).

Given the fact that graphene materials occupy an increasingly important position in biomedicine and biotechnology, the studies on their biocompatibility and biotoxicity have drawn close attention of researchers. Nevertheless, current research results in this field are mostly contradictory. Generally, because of the different preparation methods and raw materials, the obtained graphene exhibits differences in physicochemical properties such as morphology, size and surface chemistry, which are also inextricably linked to the biocompatibility of graphene (Pinto et al., 2013; Syama and Mohanan, 2016). Most studies have revealed that the biotoxicity of graphene materials (especially GO) is very limited, and usually depends on the concentration and exposure time. Furthermore, the biocompatibility of graphene can be further improved through biological or chemical functionalization (Hu et al., 2011; Justino et al., 2016).

Although graphene has good biocompatibility for mammalian cells, their inhibitory and destructive effects on bacteria and fungi also make it a high-quality material for novel green antibacterial agents (He et al., 2015). In 2010, Fan and Huang et al. first found that GO and rGO effectively inhibited the growth of *E. coli*, and confirmed the cell membrane damage of killed *E. coil* via scanning electron microscopy (SEM) (Hu et al., 2010). Various mechanisms contribute to the strong antibacterial activity of graphene, of which there are three well-recognized, including cell membrane destruction, oxidative stress and wrapping isolation (Xia et al., 2019). Cell membrane destruction refers to the physical damage caused by the cutting effect of graphene's sharp edges, which is the most important mechanism in the antibacterial effect of graphene (Ji et al., 2016). Graphene-induced oxidative stress also participates in bacterial cell damage and loss of vitality through generating reactive oxygen species (ROS), transferring charge, or oxidizing cell components directly (Gurunathan et al., 2012). On the other hand, the wrapping of graphene sheets on the bacteria can hinder the permeability and active sites of the cell membrane, resulting in decreased bacterial activity or even death (Akhavan et al., 2011).

Besides, rGO and GO have been proved to have an effective antiviral activity due to their unique monolayer structure and negative charge (Ye et al., 2015). The negative charges of GO are conducive to their mutual attraction with the positively charged virus, and then the single-layer structure and sharp edges are used to physically destroy the envelope of virus, resulting in their damage and inactivation, which usually occurs before the virus particles invade the cell. Molecular dynamics simulations were also utilized to explore the interactions between graphene and the Ebola virus protein VP40, showing that the graphene sheets could recognize and destroy the hydrophobic protein-protein interactions in VP40 (Pokhrel et al., 2017). In addition to their direct action on viruses, GO can improve their ability to inhibit viral activity by self-assembling AgNPs (Du et al., 2018) or by mimicking cell surface receptors through surface functionalization (Donskyi et al., 2019; Innocenzi and Stagi, 2020; Yang et al., 2017). Although the current level of knowledge is not sufficient to directly apply graphene to antiviral applications, it is anticipated that graphene will play an important role in the global fight against COVID-19 by being used in medical devices, personal protective equipment or mask coatings to minimize the risk of transmission (Palmieri and Papi, 2020).

In short, on account of these excellent physiochemical and biological properties, graphene nanomaterials are considered as ideal materials for constructing biosensors. However, a fatal flaw inherent in graphene is their lack of biorecognition capabilities. Therefore, it is crucial to biofunctionalize graphene with biomolecules that have the ability of recognition.

3. Bio-functionalization of graphene

There are various strategies to functionalize graphene-based nanomaterials with biomolecules, which can be divided into two main categories according to the principle of interaction: non-covalent modification and covalent functionalization. These two methods have their own strengths and weaknesses. For instance, non-covalent crosslinking has no impact on the instinct properties and structure of nanomaterials as well as the activity of biomolecules (Liu et al., 2012b). And the preparation process is simple and convenient, while the products have poor stability in complex samples and are prone to false-positive signals. The covalent method, which stabilizes biomolecules on the surface of graphene-based nanomaterials chemically, can make up for the deficiency of the non-covalent method. However, more in-depth exploration is needed to achieve higher coupling efficiency and minimize damage to the electronic structure and function of graphene. In the process of constructing biofunctionalized graphene complexes, we can choose different preparation methods according to our own requirements to achieve satisfactory sensing effects.

3.1. Non-covalent methods

In general, most biomolecules can be physically adsorbed on the surface of graphene-based nanomaterials directly without the aid of coupling agents, which is the simplest and fastest fabrication approach of biomolecule-functionalized graphene complexes. More specifically, the π–π stacking, electrostatic force, hydrogen bond and hydrophobic force between biomolecules and graphene-based nanomaterials make important contributions to promoting their interactions. By reason of the huge two-dimensional aromatic surface, graphene materials are able to interact firmly with any molecules containing aromatic rings through π–π stacking (Siontorou et al., 2019). Consequently, Most biomolecules (e.g. DNA, antibody, etc.) could be attached to the graphene surface directly (Zhang et al., 2017b). And some other biomolecules can also be adsorbed on the graphene surface by special structural design (Dowaidar et al., 2017) or modification of aromatic molecules linkers such as pyrene, porphyrin and their derivatives (Wu et al., 2015).

Electrostatic interaction also plays a important role in the interface

between biomolecules and graphene materials. GO and rGO are negatively charged because of their oxygen-containing groups, so that they are capable of adsorbing the biomolecules with positive charges (Sun et al., 2016). And neutral graphene, or even negative GO/rGO, can also be positively charged by functionalizing polymer such as polyethyleneimine, polyaniline and so on, thus electrostatically cross-linking with negatively charged biomolecules (Subramanian et al., 2014; Zheng et al., 2015). In addition, the original graphene is known to be hydrophobic, and GO has a hydrophilic edge and hydrophobic central base, so that the hydrophobic interactions between them and certain biomolecules containing hydrophobic groups also contribute to the non-covalent binding of biomolecule-graphene nanocomposites (Ling et al., 2014; Lu et al., 2012). Hydrogen bonding is the interaction between highly electronegative atoms and hydrogen atoms and has been shown to exist in the interface between biomolecules and graphene materials (Li et al., 2013a; Liu et al., 2012a; Song et al., 2015; Xue et al., 2014). These interactions usually participate in the non-covalent self--assembly of biomolecule-functionalized graphene through the coordination of two or more forces.

Non-covalent functionalization can also be achieved by in-situ synthesis (Meng et al., 2019; Zhang et al., 2017a) or modification (Saeed et al., 2017) of metal nanoparticles (e.g., AuNPs, AgNPs, PtNPs) as linkers on graphene-based nanomaterials, especially GO and rGO. The joint application of these metal nanoparticles and graphene materials can not only mediate the stable connection between graphene and biomolecules, but also enhance and amplify the transduction of sensing signals.

3.2. Covalent methods

In view of the high stability of covalent bonding, the covalent modification methods hold a great significance to functionalize graphene nanomaterials with biomolecules. The surfaces of GO and rGO are rich in oxygen-containing functional groups such as carboxyl and hydroxyl groups, making them ideal substrates for immobilizing biomolecules that also contain multiple functional groups. It is well known that most biomolecules (such as proteins, enzymes, antibodies, peptides, etc.) contain numerous amino groups, which could form stable amide bonds with carboxyl groups on GO or rGO surface under the assistance of EDC and NHS, thereby anchoring biomolecules to nanomaterials (Chiu et al., 2017; Liu et al., 2015). With regard to a few biological molecules without amino functional groups, such as nucleic acids, the similar conjugation can be achieved by labeling an amino group at their terminal (Chekin et al., 2018). Besides, it is worth noting that the introduction of polyaniline mentioned above can not only enhance the physical adsorption between biomolecules and graphene materials, but also provide amino groups for their covalent coupling (Gong et al., 2019).

Glutaraldehyde cross-linking method is also an effective covalent functionalization method, which utilizes the bifunctional group of glutaraldehyde to couple the aminated graphene materials with biomolecules (Farzin et al., 2020; Jaiswal et al., 2020). And several other bifunctional molecules, such as 1-pyrenebutyric acid N-hydroxysuccinimide ester (PNHS) and 1-pyrenebutanoic acid succinimidyl ester (PASE), can also be served as the linker of biomolecules and graphene nanomaterials (Jin et al., 2019). Their pyrene groups strongly interact with the graphene surface via π–π stacking, while the succinimidyl ester groups at the other end can undergo nucleophilic substitution reaction with the primary and secondary amines on the surface of biomolecules.

4. Graphene biosensors for pathogens

It has been confirmed that many biomolecules have the specific recognition ability for pathogens, such as nucleic acids, antibodies, peptides, bacteriophages, lectins, etc. The integration of these biomolecules with graphene biosensors not only enhances the biocompatibility and solubility of the graphene materials, but also protects them from the interference of the surrounding environment, thus improving the sensitivity of detection and the efficiency of analysis. In this section, various biomolecules-functionalized graphene biosensors for pathogen detection and their related design principles are summarized, and the comparisons between them are presented in Table 1.

4.1. Nucleic acids-functionalized graphene biosensors

Nucleic acid is a substance that plays a crucial role in storing and transmitting genetic information in the replication and synthesis of proteins. Nucleic acid probes have been developed for biosensor technology due to their superior recognition specificity, facile synthesis in vitro, excellent chemical stability, modifiable ability and good affinity for diverse platforms (Qing et al., 2020b; Qing et al., 2019b; Tyagi and Kramer, 1996). The detection of pathogens by nucleic acid-functionalized graphene biosensors is mainly based on the interaction between the whole cells or specific biomarkers (fragment genes and proteins from bacteria or viruses) and their specific recognition or complementary sequences, resulting in changes in nucleic acid structure and triggering signal output. In the following, we review graphene-based biosensors that use complementary sequences, aptamers, DNAzmyes and peptide nucleic acids for pathogen recognition by highlighting representative studies. A summary of these nucleic acids-graphene biosensors for detecting pathogens is provided in Table 2.

4.1.1. Hybridization-mediated detection of pathogens gene

Considering all organisms have their unique genetic information, DNA and RNA, as a crucial identification marker, are of great significance in the fields of clinical analysis, biomedicine, and other biological analysis (Choi et al., 2016; Choi et al., 2015; Park et al., 2015; Qing et al., 2019a). Various graphene-based biosensors constructed by hybridizing specific nucleic acid sequences of target pathogens with their complementary synthetic oligonucleotides (probes or primers) have been widely used for the detection of bacterial and viral pathogens.

Acquired immune deficiency syndrome (AIDS) is a dangerous infectious disease caused by human immune deficiency virus (HIV) infection. According to The Joint United Nations Program on HIV and AIDS (UNAIDS), the number of HIV carriers and AIDS patients worldwide had reached 37.9 million at the end of 2018, and was still increasing year by year. For the determination of the HIV-1 gene, Gong and colleagues proposed a sensitive impedimetric DNA-graphene electrochemical biosensor, which achieved a satisfactory detection limit of 2.3×10^{-14} M (Gong et al., 2017). In this study, the ssDNA capture probes were adsorbed on the surface of graphene-Nafion composite via π–π stack interaction. In the presence of HIV gene sequence, the double helix DNA formed by hybridization of probe and target oligonucleotide presented an upright state on graphene-Nafion/GCE and desorbed from

Table 1
Summary of the described graphene biosensors.

Recognition unit	Strength	Weaknesses
Nucleic acid	Artificial synthesis and easy purification of DNA recognition units, diverse signal conversion	Non-specific interference from nuclease and competitive biomolecules
Antibody	High specificity, strong recognition affinity, and real-time analysis	Susceptible to harsh conditions (e.g. high temperature and extreme pH), complicated and time-consuming production of antibodies
Peptide	Easy synthesis and high chemical/thermal stability of peptide recognition units	Limited species of functional peptides, insufficiency in specificity

Table 2
Nucleic acids-graphene biosensors for detecting pathogens.

Bio-receptors	Biosensor design	Interactions	Target	Biosensor type	Linear range	LOD	Ref.
Specific cDNA	rGO	π-π stacking interaction	H5N1 avian influenza virus gene	Electrochemistry	10 pM–100 nM	5 pM	Chan et al. (2017)
	Graphene-AuNCs	C-rich base capture probe binding	HIV gene sequences	Electrochemistry	0.1 fM–100 nM	30 aM	Wang et al. (2015)
	Graphene-Nafion composite film	π-π stacking interaction	HIV gene sequences	Electrochemistry	1.0×10^{-13}–1.0×10^{-10} M	2.3×10^{-14} M	Gong et al. (2017)
	Polyaniline-graphene	EDC/NHS	HIV gene sequences	Electrochemistry	5.0×10^{-16}–1.0×10^{-10} M	1.0×10^{-16} M	Gong et al. (2019)
	Graphene-Au nanorod-polythionine	Au–S bond and electrostatic interaction	HPV gene sequences	Electrochemistry	1.0×10^{-8}–1.0×10^{-13} M	4.03×10^{-14} M	Huang et al. (2015)
	MWCNT-NH2-IL-rGO	Glutaraldehyde	HPV gene sequences	Electrochemistry	8.5 nM–10.7 μM	1.3 nM	Farzin et al. (2020)
	Magnetic rGO-CuNCs	π-π stacking interaction	HCV subtype gene sequences	Electrochemistry	0.5–10 nM	405.0 pM	Li et al. (2020a)
	3D Graphene	Electrostatic adsorption	*S. Aureus* nuc gene sequences	Electrochemistry	1.0×10^{-12}–1.0×10^{-6} M	3.3×10^{-13} M	Niu et al. (2018b)
	rGO-AuNPs	Au–S bond	*M. tuberculosis* DNA	Electrochemistry	0.1 pM–10 nM	50 fM	Chen et al. (2017)
	APTMS-ZnO/c-GO	Glutaraldehyde	*E. coli* O157: H7 DNA	Electrochemistry	10^{-16}–10^{-6} M	0.1 fM	Jaiswal et al. (2020)
	rGO-AuNPs	Au–S bond	*M. tuberculosis* DNA	Electrochemistry	0.1 fM–10^{-6} M	0.1 fM	Mogha et al. (2018)
	GO	π-π stacking interaction	Ebola virus gene	Fluorescence	30 fM–3 nM	1.4 pM	Wen et al. (2016)
	GO	π-π stacking interaction and hydrogen bonding	Influenza virus H3N2 hemagglutinin gene	Fluorescence	37–9400 pg	3.8 pg	Jeong et al. (2018)
	GO	π-π stacking interaction	*B. anthracis* pagA gene	Fluorescence	0.625–2.5 μM	0.625 μM	Ziółkowski et al. (2020)
	GO	π-π stacking interaction	Methicillin-resistant *S. aureus* harboring 16S rRNA	Fluorescence	1–30 nM	0.02 nM	Ning et al. (2018)
	GO	Hydrophobic and π–π stacking interactions	*Chlamydia trachomatis* DNA	Fluorescence	0–1 nM	6.7 pM	Lee et al. (2019)
	Graphene-AuNPs	Au–S bond	*S. aureus* gene sequences	Surface acoustic wave (SAW)	0–10 nM	12.4 pg/mL	Ji et al. (2020)
Aptamers	rGO/MoS2	EDC/NHS	L1-major capsid protein of HPV	Electrochemistry	0.2–2 ng/mL	0.1 ng/mL	Chekin et al. (2018)
	Graphene-AuNPs	Streptavidin-biotin interaction	Norovirus	Electrochemistry	100 pM–3.5 nM	100 pM	Chand and Neethirajan (2017)
	rGO-CNT	–	*S. Typhimurium*	Electrochemistry	10–10^8 CFU/mL	10 CFU/mL	Appaturi et al. (2020)
	GO	π-π stacking interaction	*P. aeruginosa*	Electrochemistry	1.2–1.2×10^7 CFU/mL	12 CFU/mL	Shahrokhian and Ranjbar (2019)
	rGO-AuNPs	EDC/NHS	LPS from *E. coli* 055: B5	Electrochemistry	–	30 fg/mL	Pourmadadi et al. (2019)
	rGO-azophloxine	π-π stacking interaction	*S. Typhimurium*	Electrochemistry	10–10^8 CFU/mL	10 CFU/mL	Muniandy et al. (2017)
	rGO-MWCNT	EDC/NHS	*Salmonella*	Electrochemistry	75–7.5×10^5 CFU/mL	25 CFU/mL	Jia et al. (2016)
	UiO-67/Graphene	Phosphate and UiO-67 interaction	*S. Typhimurium*	Electrochemistry	2×10^1–2×10^8 CFU/mL	5 CFU/mL	Dai et al. (2019)
	Graphene	Pyrene phosphoramidite linker	*E. coli*	Electrochemistry	10^2–10^6 CFU/mL	10^2 CFU/mL	Wu et al. (2017)
	Bridged rebar graphene	Poly-L-lysine	*E. coli* O78:K80:H11	Electrochemistry	10–10^6 CFU/mL	10 CFU/mL	Kaur et al. (2017)
	GO	π-π stacking interaction	LPS	Fluorescence	10–500 ng/mL	8.7 ng/mL	Wen et al. (2019)
	GO	π-π stacking interaction	*S. enteritis*	Fluorescence	10^2–10^7 CFU/mL	25 CFU/mL	Chinnappan et al. (2018)
	GO	Hydrophobic and π–π stacking interactions	Secretory protein (Ag85A) of *M. tuberculosis*	Fluorescence	5–200 nM	1.5 nM	Ansari et al. (2018)
	rGO	Hydrophobic and π–π stacking interactions	LPS from *E. coli* 055: B5	Fluorescence	50-10^6fM and 50–5 × 10^4fM for water sample and serum	7.9 fM and 8.3 fM for water sample and serum sample	Niu et al. (2018a)
	GO			Fluorescence	–	38.7, 88.0, 154 ng/mL	Ye et al. (2019)

(*continued on next page*)

Table 2 (*continued*)

Bio-receptors	Biosensor design	Interactions	Target	Biosensor type	Linear range	LOD	Ref.
		π-π stacking and electrostatic interaction	LPSs from *S. Typhimurium*, *P. aeruginosa* 10 and *E. coli* 055: B5				
	Fe3O4-AuNPs-GO	Au–S bond	*V. parahaemolyticus*	Surface-enhanced Raman scattering	1.4×10^2–1.4×10^6 CFU/mL	14 CFU/mL	Duan et al. (2017)
Peptide nucleic acids	Graphene-polyaniline	Electrostatic interaction	HPV type 16 DNA	Electrochemistry	10–200 nM	2.3 nM	Teengam et al. (2017)
	GO-CdS QDs	EDC/NHS	*M. tuberculosis* DNA	Electrochemistry	10^{-11}–10^{-7}M	8.948×10^{-13} M	Zaid et al. (2017)
	rGO-TEMPO-NCC	EDC/NHS	*M. tuberculosis* DNA	Electrochemistry	10^{-13}–10^{-8}M	3.14×10^{-14} M	Zaid et al. (2020)

the sensing surface, resulting in the changes of graphene-Nafion interfacial property, which could be monitored by electrochemical impedance spectrum (EIS) (Fig. 1A).

Modifiability of DNA oligonucleotides also provides many other means for determining specific gene sequences in bacterial and viral pathogens. For example, Wen et al. described a novel fluorescence biosensor based on rolling circle amplification (RCA) and the fluorescence quenching property of GO, which allowed sensitive and selective detection of Ebola virus (EBOV) gene with the LOD of 1.4 pM (Wen et al., 2016). Prior to the detection, the FAM-labeled detection probes were adsorbed on the surface of GO, and almost no fluorescence could be detected in the system. While the addition of trigger chains (EBOV gene) set RCA reaction in motion, and dsDNA were formed between the RCA products and detection probes, enabling FAM labeled probes to desorb from GO and restore fluorescence (Fig. 1B). In another study, a sensitive and specific fluorescence biosensor was fabricated relied on the use of flap endonuclease-assisted amplification and GO-based fluorescence signaling, which could be utilized for the detection of DNA from *Chlamydia trachomatis* with the LOD of 6.7 pM and had a reliable application in human serum (Lee et al., 2019).

Recently, Ji and colleagues developed a graphene/AuNPs based Love wave biosensor for the detection of *S. aureus* gene sequences (Fig. 1C) (Ji et al., 2020). Surface acoustic wave (SAW) sensor is a kind of piezoelectric mass sensor, which is sensitive to surface mass loading since the loading has a great influence on the propagation of the acoustic wave (Ballantine Jr et al., 1996). Among the various SAW sensors, Love wave sensor is especially suitable for the biological detection of liquid phase. In this work, AuNPs were deposited onto the graphene film by the electron-beam evaporation (EBE) process and the ssDNA probes were immobilized by Au–S bonding. When the target sequences were present,

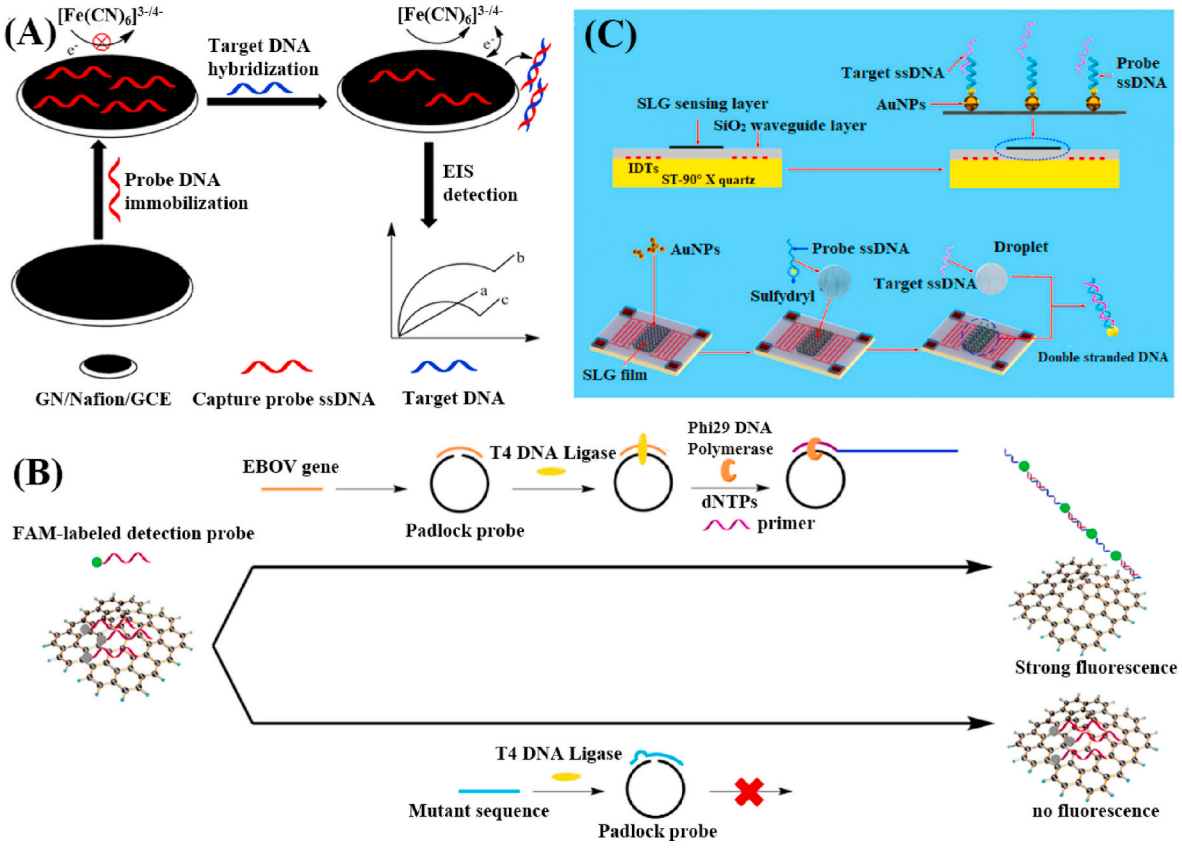

Fig. 1. (A) Schematic illustration of the construction of the impedimetric DNA-Graphene biosensor for HIV gene detection. (Reproduced with permission from Ref. (Gong et al., 2017). Copyright 2017, Elsevier). (B) Working principles of the DNA-GO fluorescence biosensor for the detection of EBOV gene. (Reproduced with permission from Ref. (Wen et al., 2016). Copyright 2016, Elsevier). (C) Schematic diagram of a Love wave biosensor and the detection process of *S. aureus* gene sequence. (Reproduced with permission from Ref. (Ji et al., 2020). Copyright 2020, American Chemical Society).

the amplitude of the Love wave and phase velocity would be changed. This sensor had an excellent sensitivity to *S. aureus* gene sequences with a low detection limit of 1.86 M and great potential in clinical testing and diagnosis.

4.1.2. Aptamer recognition-mediated detection of pathogen cells

In addition to nucleic-hybridization assays, aptamers that can interact with individual pathogen cells or specific proteins secreted by the pathogen are also commonly used as recognition elements of graphene-based biosensors for detecting bacteria and viruses. Aptamer is a small segment of oligonucleotide sequence (RNA or DNA) selected via Systematic Evolution of Ligands by Exponential Enrichment (SELEX) method in vitro, which can bind to the corresponding target molecule with strong affinity and high specificity by folding into unique three-dimensional structures. After a series of screening and enrichment, aptamers display a high sensitivity comparable to antigen-antibody reactions and are therefore known as chemical antibodies (Song et al., 2008). Moreover, in contrast to the protein-based antibodies, aptamers possess higher chemical stability, smaller size, easy availability, and a wide range of targets (from inorganic ions to organic macromolecules and even intact cells) (Iliuk et al., 2011). Several aptamers against pathogens or pathogen biomarkers have been proposed to help detect specific bacteria or viruses, including *S. enterica, S. aureus,* norovirus and so on (Appaturi et al., 2020; Chand and Neethirajan 2017; Hernández et al., 2014). Therefore, biosensors constructed with aptamer-modified graphene materials have great potential prospects for the detection of pathogenic microorganisms.

Currently, most of the pathogen aptamers that have been selected are whole-cell aptamers, which take the whole pathogen cell as the target (McConnell et al., 2019). The biosensors constructed by this kind of aptamer for detecting pathogens do not require sample processing (for example, bacterial or viral lysis) to release intracellular components, thereby reducing the time and cost of analysis (Hoyos-Nogués et al., 2018). For example, an electrochemical device was designed for the determination of whole bacteria cell, *Pseudomonas aeruginosa*, which immobilized the aptamers on the surface of engineered zeolitic imidazolate framework-8 (ZIFs-8) via carboimide cross-linking (Shahrokhian and Ranjbar, 2019). Ferrocene-graphene oxide (Fc-GO) could be adsorbed on the surface of aptamer sensor due to π-π stacking between GO with *P. aeruginosa* aptamers, which would be inhibited by the specific binding of *P. aeruginosa* and aptamers, resulting in signal output and monitored by the differential pulse voltammetry (DPV). (Fig. 2A). The proposed whole-cell electrochemical aptasensor exhibited a wide linear dynamic range (1.2×10^1-1.2×10^7 CFU/mL) and low detection limit (12 CFU/mL) with satisfactory repeatability.

Aptamers selected using living cells as targets mean that all biomolecules on the cell surface can be potential targets for aptamer binding, while that may lead to the selection of aptamers that bind to non-specific structures on the cell surface, thereby affecting the specificity of aptamers. Therefore, aptamers obtained utilizing certain pathogen biomarkers are of great concern since they can bind to the specific targeting molecules on the cell, thus minimizing the risk of false-positive signals caused by non-specific aptamers (McConnell et al., 2019). Based on the specific interaction of HPV-16 L1 protein and its aptamers, Chekin et al. proposed the porous rGO-molybdenum sulfide (prGO--MoS_2) modified glassy carbon (GC) electrical interfaces as electrochemical transducers for the determination of human papillomavirus (HPV) (Chekin et al., 2018). A low detection limit of 0.1 ng/mL (1.75 pM) was achieved in the range of 0.2–2 ng/mL (3.5 pM–35.3 pM) and the study of cross-reactivity proved that the method was still highly selective in the presence of interfering substances such as HPV-16 E6. Lipopolysaccharide (LPS), also known as endotoxin, is the main component of gram-negative bacteria outer membrane and is a hypertoxic inflammatory stimulator released when bacterial cells die. Liu' group developed a microfluidic chip based on continuous injection-electrostacking (CI-ES) by combining rGO with FAM-aptamer, which was not only able to be used for sensitive, efficient and specific detection of LPS, but also could distinguish gram-negative bacteria from gram-positive bacteria and fungus (Fig. 2B) (Niu et al., 2018a).

4.1.3. DNAzyme cleavage-mediated detection and gene silencing

DNAzmyes, as one of the two main members of functional nucleic acid, are different from the recognition and binding between aptamers and target molecules, which mainly fold appropriately and/or carry out enzymatic reactions under the auxiliary role of the target (Zaouri et al., 2019). DNA enzymes are generally divided into two forms: one is cis-acting DNAzymes, whose enzymes and substrate chains are linked by DNA hairpins to form a whole, and another is trans-acting DNAzymes, which require a hybridization process to combine the enzymes and substrate chains prior to the reaction (Aguirre et al., 2013). A variety of DNAzymes specific to bacterial and viral targets have been developed and applied for biosensors designing since Li's group isolated an RNA-cleaving fluorescent DNAzmye with high specificity for *E. coli* from DNA libraries for the first time in 2011 (Ali et al., 2011).

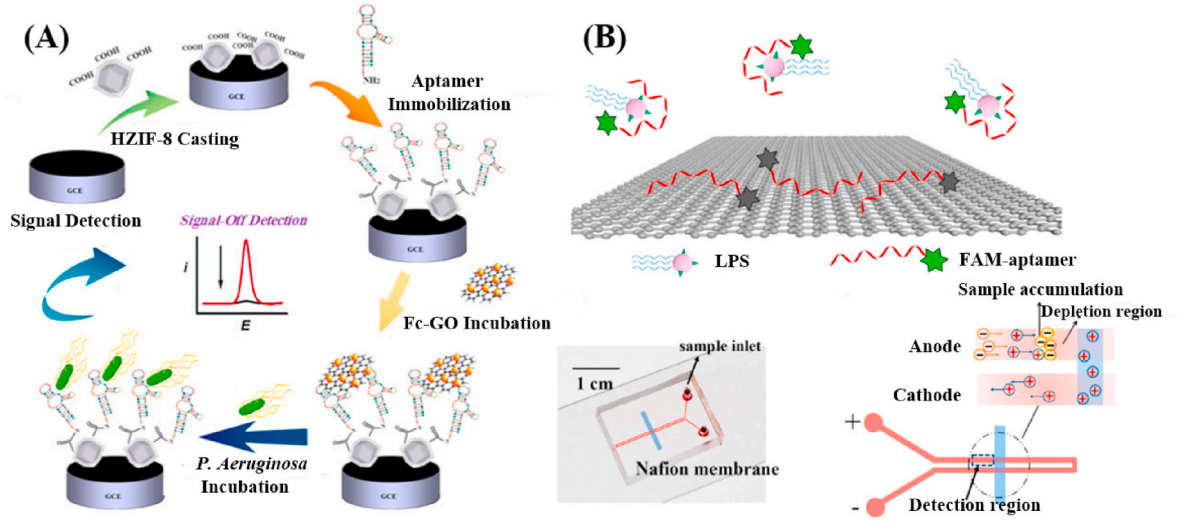

Fig. 2. (A) Schematic diagram of the fabrication of aptasensor and the detection of *P. aeruginosa*. (Reproduced with permission from Ref. (Shahrokhian and Ranjbar, 2019). Copyright 2019, American Chemical Society). (B) Mechanism of determination of LPS by coupling FAM-aptamer and rGO based on the CI-ES method using a microfluidic biochip. (Reproduced with permission from Ref. (Niu et al., 2018a). Copyright 2018, American Chemical Society).

Aware of the superiority of nanomaterial-assisted biosensors, Li's group took advantage of graphene's ability to non-covalently adsorb DNA and *E. coli*'s specific DNAzyme, building a fluorescent biosensor that could detect *E. coli* real-timely, sensitively and highly selectively (Liu et al., 2018b). In this work, the exposure of DNAzyme/graphene composites to the samples containing target *E. coli* induced the cleavage of fluorophore-labeled substrate chains, resulting in a dramatic recovery of the fluorescence signal in the solution (Fig. 3A). In addition, Kim et al. designed a biosensor based on FAM-DNAzymes/GO complexes, in which the target hepatitis C virus (HCV) gene was applied as the substrate chain of DNAzyme (Kim et al., 2013) (Fig. 3B). In brief, GO was served as an intracellular transport carrier and fluorescence quenching agent to deliver FAM-DNAzymes to human liver cells. In the presence of the target gene HCV NS3 mRNA, the formation of double-stranded structures and desorption from GO restored the fluorescence of FAM-DNAzymes, followed by catalytic cleavage of HCV NS3 mRNA. Therefore, this method could not only monitor the existence and situation of the HCV gene in living cells, but also down-regulate the expression of the HCV NS3 protein by catalytic cleavage of the substrate sequence, thereby inhibiting the replication of HCV in host cells. Although the sensitivity of these platforms is not yet comparable to that of electrochemical biosensors, they show a new strategy to detect pathogens in the realms of food safety, infectious disease diagnosis and environmental monitoring.

4.1.4. Peptide nucleic acids-mediated improvement of detection performance

Peptide nucleic acid (PNA) is a kind of nucleic acid analogs that replaces the backbone of sugar phosphate with a synthetic peptide backbone formed by N-(2-amino-ethyl)-glycine unit. The superior hybridization performance and chemical stability of PNA make it very appropriate for sensing specific nucleic acid sequences in the multi-component environment and even in the whole cell. On the one hand, PNAs are uncharged achiral molecules with the ability to resist hydrolytic enzymatic cleavage, thus exhibiting high stability in complex environments (Ray and Nordén, 2000). And on the other hand, despite a significant structural change compared to natural DNA or other DNA analogs, PNAs are still capable of recognizing and binding specific DNA or RNA sequences following the Watson-Crick hydrogen bonding principle (Egholm et al., 1993). Furthermore, owing to the absence of phosphate groups in the PNAs backbone, the combination of PNA to DNA (or RNA) will not be affected by electrostatic repulsion, which makes the DNA/PNA (or RNA/PNA) hybrids present more remarkable thermal stability and distinct ion strength effects than the ordinary double-stranded structure (Saadati et al., 2019).

Recently, a large number of researches have demonstrated that PNAs-based biosensors expand the detection pathway of pathogenic bacteria and viruses, and their performance would be effectively enhanced by the introduction of graphene nanomaterials. Teengam et al. developed a low-cost, highly efficient paper-based PNA-graphene biosensor that is expected to be used in screening and monitoring type 16 HPV DNA for early diagnosis of cervical cancer (Teengam et al.,

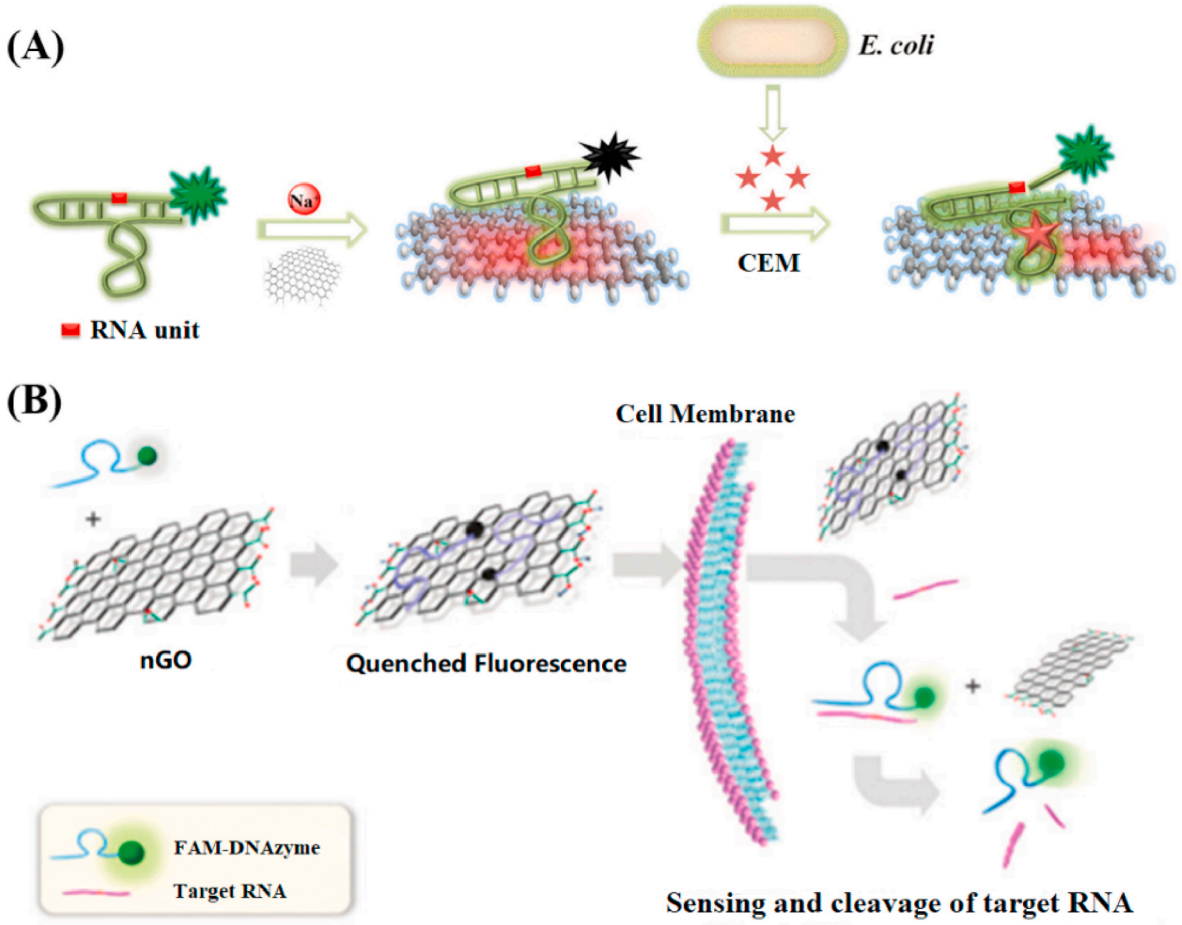

Fig. 3. (A) Schematic diagram of the fluorogenic graphene-DNAzyme biosensor for the determination of *E. coli.* (Reproduced with permission from Ref. (Liu et al., 2018b). Copyright 2018, Cambridge Core). (B) Principle of detection and knockdown of HCV RNA in mammalian cells based on FAM-DNAzyme and nGO. (Reproduced with permission from Ref. (Kim et al., 2013). Copyright 2013, Royal Society of Chemistry).

2017). This device immobilized the anthraquinone-labeled pyrrolidinyl PNA probes (AQ-PNA) on polyaniline-modified graphene (G-PANI) electrode surface via electrostatic attraction, and employed the square wave voltammetry to monitor the electrochemical signal degradation caused by the hybridization of PNA and cDNA targets (Fig. 4A). The results showed that this method had a low detection limit of 2.3 nM for HPV type 16 DNA in a linear range of 10–200 nM and revealed good selectivity against non-complementary DNA such as HPV types 18, 31 and 33 DNA.

Mycobacterium tuberculosis, the bacterium that can cause tuberculosis (TB), is regarded as an extremely dangerous pathogen, so that it is critical to detect them early for preventing TB epidemic. Issa's group fabricated a electrochemical PNA biosensor with extremely high sensitivity for the detection of *M. Tuberculosis* (Fig. 4B) (Zaid et al., 2017). In this work, PNA probes were anchored on the surface of the screen-printed carbon electrode deposited with NH_2-GO/QDs via the EDC/NHS chemistry. Methylene blue (MB) and DPV were applied as electrochemical indicators and signal monitoring techniques, respectively. This PNA-GO sensor showed unexceptionable sensitivity and selectivity, could detect *M. Tuberculosis* DNA below the level of sub picomolar, and had the ability to distinguish between complementary and non-complementary sequences clearly. Recently, they modified the above PNA-GO biosensor for more sensitive detection of *M. Tuberculosis* DNA by replacing NH_2-GO/QDs nanocomposites with amine-functionalized reduced graphene oxide (NH_2-rGO) and 2,2,6,6-tetramethylpiperidin-1-yl) oxyl nanocrystalline cellulose (TEMPO-NCC) nanomaterials (Fig. 4C) (Zaid et al., 2020). According to the results, this improved PNA biosensor showed a more extensive linear range (10^{-13}-10^{-8} M) and a lower detection limit (3.14×10^{-14} M) than the previous study.

4.2. Antibody-functionalized graphene biosensors

Although aptamers can be regarded as an alternative to antibodies in the field of biosensing, antibodies, as a conventional biorecognition molecule, still have their particular merits and unshakable status. The unique biological activity of antibodies makes them play an important role in the diagnosis, prevention and treatment of diseases and basic research. Traditionally, antibodies are immobilized on the immunoassays surfaces by physical adsorption, such as classic 96-microwell plates and colloidal gold test strips, thereby relying on the specific binding of antibodies to antigens for detection (Zhou et al., 2020). These methods have been widely used in clinical diagnosis and biological detection, while there are still obstacles with time-consuming process and low sensitivity. Consequently, a kind of novel biosensor based on the interface between antibodies and graphene nanomaterials gradually enters the researchers' field of vision. In this part, we mainly discuss graphene biosensors using antibodies as biorecognition molecules for the detection of pathogenic bacteria and viruses and the summary of detection related is listed in Table 3.

On account of diverse and different epitopes in the natural antigen molecules, stimulating the body's immune system with these antigens could simultaneously activate the cloning of multiple B lymphocytes, thus producing multiple antibodies against different epitopes, which are called as polyclonal antibodies. Polyclonal antibodies have received much attention due to their simple preparation, wide source and comprehensive function, etc. (Leonard et al., 2003), and have been commonly used in the construction of biofunctionalized graphene sensors to detect pathogens. For example, Islam and colleagues conjugated the polyclonal antibodies (anti-p24 for HIV, anti-cardiac troponin 1 for cardiovascular disorders, and anti-cyclic citrullinated peptide for rheumatoid arthritis) to NH_2-graphene via the EDC/NHS carbodiimide chemistry, constructing an ingenious functionalized graphene transistor for the detection of HIV and associated diseases (Fig. 5A) (Islam et al., 2019). Thakur et al. designed a rGO-based field-effect transistor (FET) passivated with Al_2O_3 ultrathin layer for real-time detection of *E. coli* bacteria, which anchored the *E. coli* serotype O/K polyclonal antibody probes onto the surfaces of AuNPs-rGO with the help of EDC and NHS

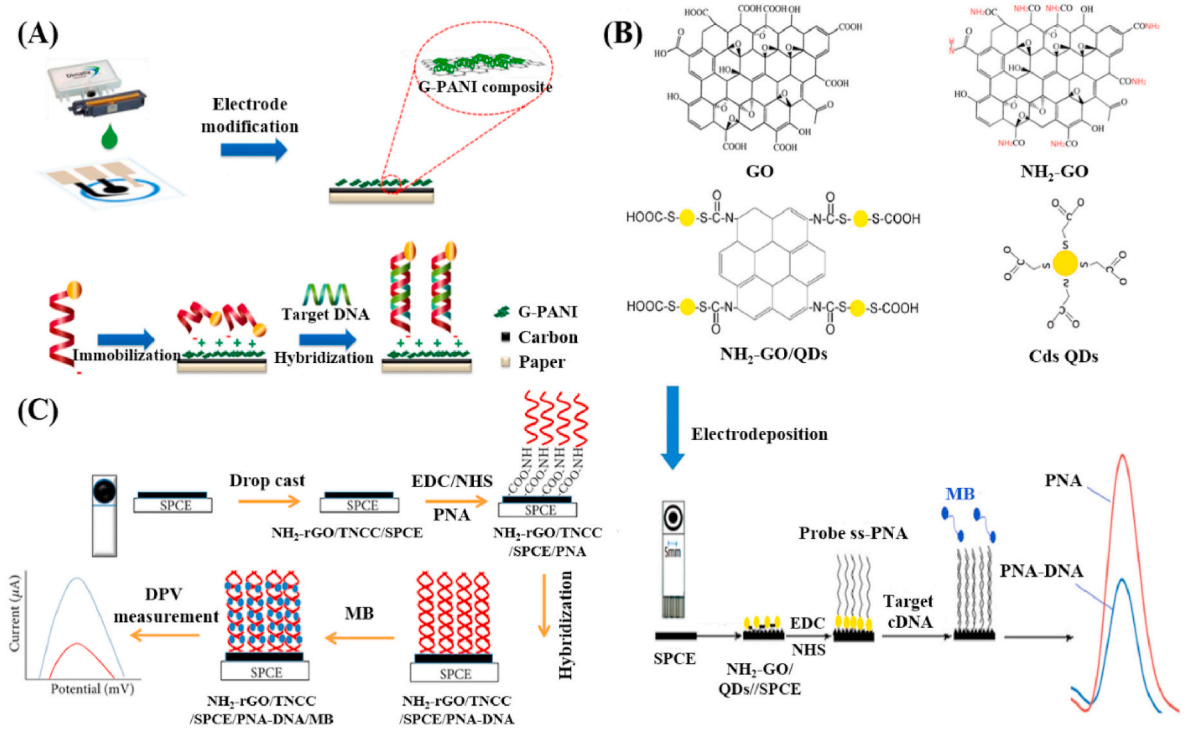

Fig. 4. (A) Mechanism illustration of the preparation and detection procedure of paper-based electrochemical PNA-Graphene biosensor. (Reproduced with permission from Ref. (Teengam et al., 2017). Copyright 2017, Elsevier). (B) Illustration of the preparation strategy of NH_2-GO/QDs complex and working procedure of *M. tuberculosis* detection. (Reproduced with permission from Ref. (Zaid et al., 2017). Copyright 2017, Elsevier). (C) The stepwise diagram for the construction of the PNA-rGO electrochemical biosensor. (Reproduced with permission from Ref. (Zaid et al., 2020). Copyright 2020, Hindawi).

Table 3
Antibody-graphene biosensors for detecting pathogens.

Antibody	Biosensor design	Interactions	Target	Biosensor type	Linear range	LOD	Ref.
Monoclonal antibodies (H5N1 and H1N1)	GO	Drop-casting	H5N1 and H1N1 antigens	Electrochemistry	25–500 pM	H5N1: 9.4 pM; H1N1: 8.3 pM	Veerapandian et al. (2016)
Anti-EBOV antibody	rGO	PASE linker	Ebola virus glycoprotein	Electrochemistry	2.4×10^{-12}–1.2×10^{-7} g/mL	2.4 pg/mL	Jin et al. (2019)
Anti *E. coli* O157: H7 antibodies	rGO-NR-Au @ Pt	Au–N and Pt–N bond	*E. Coli* O157: H7	Electrochemistry	4.0×10^{2}–4.0×10^{8} CFU/mL	91 CFU/mL	Zhu et al. (2018)
anti-fimbrial *E. coli* antibody	rGO/PEI	EDC/NHS	Uropathogenic *E. coli* UTI89 bacteria	Electrochemistry	10–10^{4} CFU/mL	10 CFU/mL	Jijie et al. (2018)
AIV H7-polyclonal antibodies and H7-monoclonal antibodies	AuNPs-Graphene and AgNPs-G	Au-amine bond and EDC/NHS	avian influenza virus (AIV) H7	Electrochemistry	1.6×10^{-3}-16 ng/mL	1.6 pg/mL	Huang et al. (2016)
S. pullorum secondary antibody	AuNPs-rGO	Au–S bond	*Salmonella pullorum*	Electrochemistry	10^{2}–10^{6} CFU/mL	89 CFU/mL	Fei et al. (2016)
S. typhimurium antibody	GO-cMWCNTs	EDC/NHS	*S. Typhimurium*	Electrochemistry	10–10^{7} CFU/mL	0.376 CFU/mL	Singh et al. (2018)
Mouse anti-flavivirus group antigen monoclonal antibody	Au/MNP-Graphene	EDC/NHS	Norovirus-like particle	Electrochemistry	0.01 pg/mL–1 ng/mL	1.16 pg/mL	Lee et al. (2017)
Anti-Zika NS1 antibody	Graphene	NHS surface chemistry	Zika viral nonstructural protein 1	Electrochemistry	–	0.45 nM	Afsahi et al. (2018)
PEDV-2C11 antibody	AuNP–MoS2-rGO	Adsorption	Porcine epidemic diarrhea virus	Electrochemistry	$82.5–1.65 \times 10^{4}$ $TCID_{50}$/mL	–	Li et al. (2020b)
DENV 4G2 antibody	GO	Electrostatic bond	Dengue virus	Electrochemistry	$1–2 \times 10^{3}$ PFU/mL	0.12 PFU/mL	Navakul et al. (2017)
anti-HIV p24 antibody	Graphene	EDC/NHS	HIV antigen	Electrochemistry	1 fg/mL–1 μg/mL	100 fg/mL	Islam et al. (2019)
Anti-*E. coli* antibody	rGO	EDC/NHS	*E. coli*	Electrochemistry	10^{3}–10^{5} CFU/mL	10^{3} CFU/mL	Thakur et al. (2018)
Goat anti-*E. coli* O157: H7 antibody	AuNPs-Graphene	Physical adsorption between antibodies and AuNPs	*E. coli* O157: H7	Electrochemistry	10^{2}–10^{8} CFU/mL	10^{2} CFU/mL	You et al. (2020)
Rabbit anti-*E. coli* antibody	AuNPs-Graphene	Biotin-streptavidin combination	*E. coli* K12 ER2925	Electrochemistry	$2.4 \times 5–2.4 \times 5^{6}$ CFU/mL	12 CFU/mL	Zhao et al. (2020)
Anti-*E. coli* O157: H7 antibodies	NH2-GO	EDC/NHS	*E. coli* O157: H7	Electrochemistry	2.2×10^{2}–2.2×10^{8} CFU/mL	2 CFU/mL	Gupta et al. (2019)
E. coli O157: H7-specific-antibodies	Graphene nanoplatelets (GNPs) or monolayered-graphene (MG)	1-Pyrenebutanoic acid succinimidyl ester linker	*E. coli* O157: H7	Electrochemistry	GNPs: 10^{2}–10^{6} cells/ml MG: 0-10^{7} cells/ml	GNPs: 100 cells/ml MG: 10 cells/ml	Pandey et al. (2017a)
Anti *E. coli* O157: H7 antibody	rGO-CysCu	EDC/NHS	*E. coli* O157: H7	Electrochemistry	10–10^{8} CFU/mL	3.8 CFU/mL	Pandey et al. (2017b)
McAb against *S. enteritidis* flagellin	Graphene	Van der Waals forces, electrostatic, hydrophobic interactions	*S. enteritidis*	Colorimetry	0–10^{8} CFU/mL	10^{3} CFU/mL	Bu et al. (2019)
E. coli monoclonal antibody	GO or rGO	Physical absorption	*E. coli* O157: H7	Colorimetry	10^{4}–10^{7} CFU/mL	10^{5} CFU/mL	Shirshahi et al. (2019)
anti-NoV Ab (NS-14)	AuNPs-Graphene	EDC/NHS	norovirus-like particles	Colorimetry	100 pg/mL–10 μg/mL	92.7 pg/mL	Ahmed et al. (2017)
Antihuman IgG Ab	GO cellulose nanopaper-QDs	Conjugation process	*E. coli*	Photoluminescence	10–10^{6} CFU/mL	55 CFU/mL	Cheeveewattanagul et al. (2017)
HBsAg monoclonal antibody	GO-GNRS	EDC/NHS	Hepatitis B surface antigen	Surface-enhanced Raman scattering	1–1000 pg/mL	0.05 pg/mL	Liu et al. (2018c)
DENV E-protein monoclonal antibody	CdS–NH2GO	EDC/NHS	Dengue virus E-protein	Surface plasmon resonance	0.0001–10 nM	0.001 nM	Omar et al. (2019)
Anti-CT	Graphene–polypyrrole	π–π interactions	Cholera toxin	Surface plasmon resonance	0.004–4 ng/mL	4 pg/mL	Singh et al. (2015)

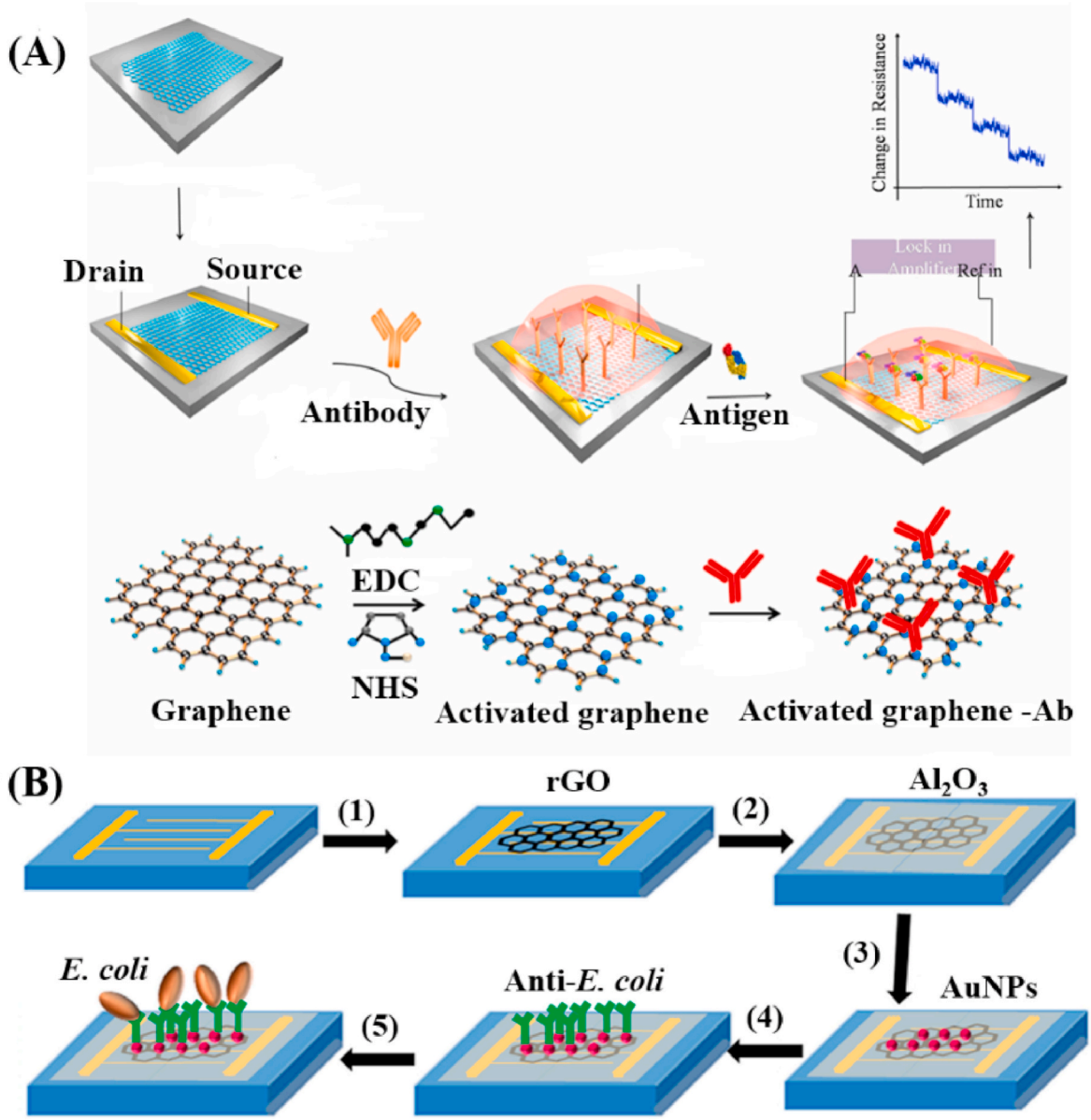

Fig. 5. (A) Schematic depicting the antibody-graphene immunosensor fabrication and the antibody-graphene composite preparation using the carbodiimide strategy. (Reproduced with permission from Ref. (Islam et al., 2019). Copyright 2019, Elsevier). (B) Schematic illustration of the fabrication steps of anti-*E. coli*/AuNPs/Al_2O_3/rGO FET biosensor. (Reproduced with permission from Ref. (Thakur et al., 2018). Copyright 2018, Elsevier).

(Fig. 5B) (Thakur et al., 2018). This FET sensor could detect a single *E. coli* cell in a microliter sample volume within 50 s, and was further demonstrated the successful application in river water.

However, polyclonal antibodies have several serious shortcomings, including low specificity and easy cross-reaction, thereby limiting the scope of their applications. The ideal method to solve these drawbacks is to prepare antibodies that recognize the specificity of a single epitope so that the preparation technology of monoclonal antibody was established. Monoclonal antibody technology is a milestone breakthrough of immunology in the 20th century and provides a new method for the diagnosis and treatment of diseases in clinical applications. The strong specificity, high purity and homogeneity of monoclonal antibodies have greatly promoted the interest of researchers, and have been widely used in the detection and diagnosis of pathogenic microorganisms, tumors, immune cells, hormones and cytokines. With the development of monoclonal antibodies, the graphene-based immunosensors for bacterial and viral pathogens have become more specific, sensitive, repeatable and reliable.

Pandey and colleagues fabricated a highly sensitive electrochemical immunosensor by modifying the monoclonal antibody (EcAb) on the graphene-wrapped copper oxide-cysteine hierarchical structure (rGO-CysCu) surfaces (Fig. 6A) (Pandey et al., 2017b). The proposed sensing platform not only had high selectivity and sensitivity (LOD: 3.8 CFU/mL) for the detection of *E. coli* O157: H7, but also could be utilized to distinguish the *E. coli* O157: H7 cells from the non-pathogenic *E. coli* (DH5) and other bacterial cells in the synthetic samples. In order to evaluate the characteristics of materials and equipment through large-scale production and to approach potential requirements for field diagnostic equipment, Afsahi et al. constructed a novel biosensor using a commercially available graphene biosensor chip modified with anti-Zika NS1, which allowed sensitive and specific determination of Zika viral nonstructural protein 1 (ZIKV NS1) with a low LOD of 0.45 nM, and showed no cross-reactivity in the presence of related co-transmitting viral antigen such as Japanese encephalitis NS1 (Afsahi et al., 2018).

So far, a large number of literature reports indicate that most biosensors constructed from graphene materials combined with

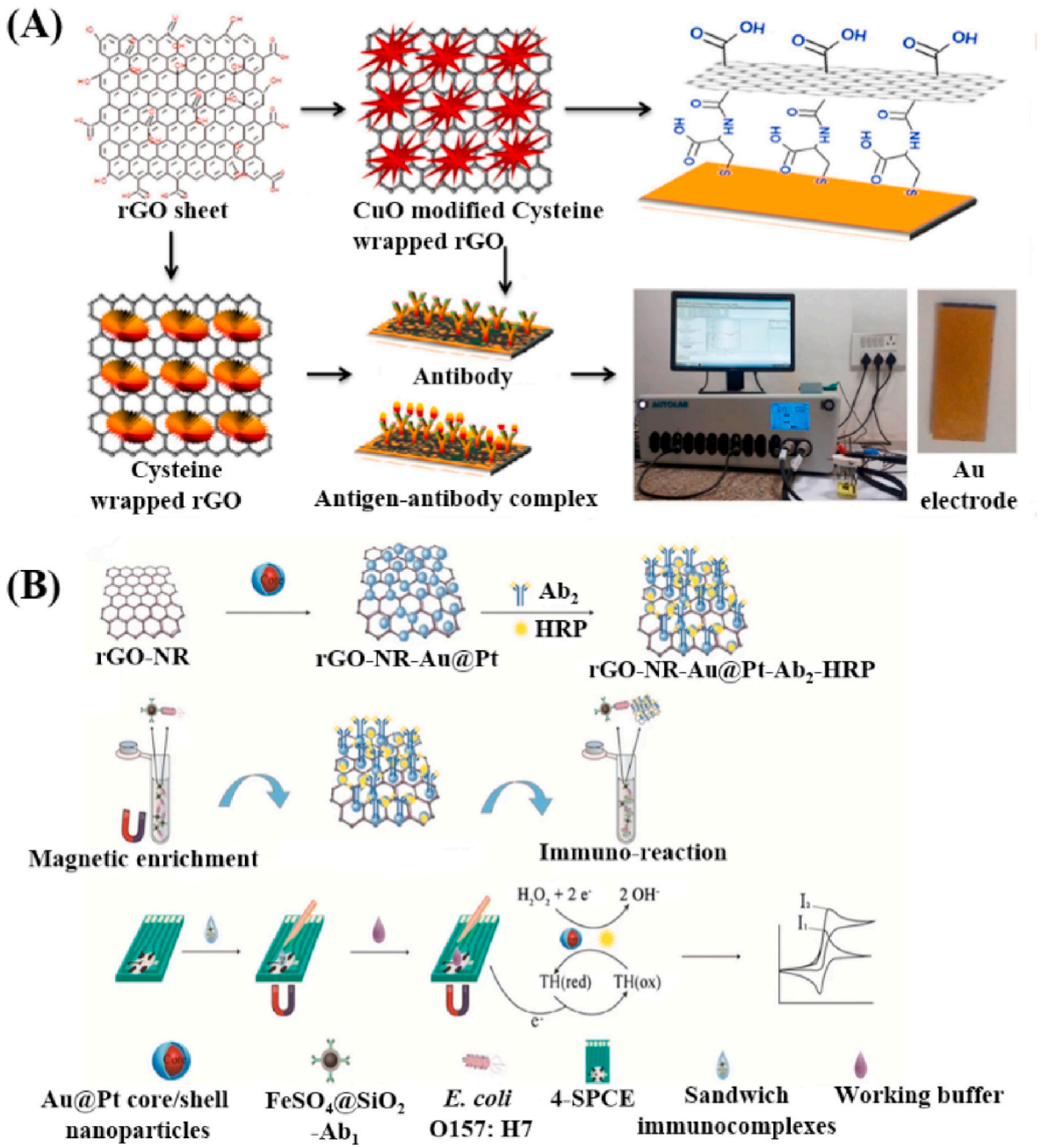

Fig. 6. (A) Schematic diagram of the preparation of rGO-CysCu and rGO-Cys self-assembling on the gold electrode and subsequent fabrication of immunosensor. (Reproduced with permission from Ref. (Pandey et al., 2017b). Copyright 2017, Elsevier). (B) Formation steps of rGO-NR-Au@Pt-Ab_2-HRP composite and detection mechanism of the electrochemical immunoassay of *E. coli* O157: H7. (Reproduced with permission from Ref. (Zhu et al., 2018). Copyright 2018, Springer). (For interpretation of the references to color in this figure legend, the reader is referred to the Web version of this article.)

monoclonal antibody are capable of achieving high selective and sensitive detection. However, the high specificity of monoclonal antibodies for a single epitope also presents a challenge that it is unable to form the binding of antigens and antibodies if the epitope is blocked or destroyed, resulting in false-negative signals.

Among the immunoassays based on the specific binding of antigen and antibody, the double antibody sandwich assay has the highest sensitivity and specificity due to the use of two matching antibodies (Quinton et al., 2012), and thus has universal applicability. By introducing graphene nanomaterials, sandwich immunoassay is no longer limited to the ordinary enzyme-linked colorimetric method, but can also be used for more advanced immunoassay methods such as optical and electrochemical sensors. Huang and colleagues designed a novel electrochemical immunosensor based on a sandwich-type immunoassay format for the quantitative determination of avian influenza virus H7 (AIV H7) (Huang et al., 2016). In this work, the H7 monoclonal antibody (MAb) was modified on the gold electrode coated with AuNPs-Graphene nanocomposite materials via Au-amine bonds, and the H7 polyclonal antibody (PAb) was attached to AgNPs-Graphene surfaces through the EDC/NHS chemistry. In the presence of AIV H7, the Graphene-AgNPs-PAb/AIV H7/MAb-AuNPs-Graphene sandwich structure was formed on the electrode, and the linear sweep voltammetry (LSV) peak current of the immunosensor enhanced with the increase of antigen concentration. Similarly, the formation of Fe_3O_4@SiO_2-Ab_1/*E. Coli* O157: H7/rGO-NR-Au@Pt-Ab_2-HRP sandwich immunocomplex was also used for the electrochemical immunoassay of *E. coli*

O157: H7 (Fig. 6B) (Zhu et al., 2018). Considering that these methods still require several long incubation/washing steps and that analysis time is a key factor in practical application, accordingly, continuous efforts are still needed to develop more sensitive and simpler antibody-graphene biosensors.

4.3. Peptide-functionalized graphene biosensors

Recently, owing to the high affinity displayed between peptide-based biorecognition molecules and their targets, peptides have been used as recognition elements to construct biosensors in many applications. In general, peptides are oligopeptides developed from the binding domain of proteins, or oligopeptides screened by phage display technology. They possess a variety of superiority compared to antibodies, such as low molecular weight, easy synthesis and modification, and strong chemical/thermal stability. Similar to nucleic acids and antibodies, plenty of studies have shown that short-chain peptides can also be combined with graphene via physical adsorption and chemical coupling. Thanks to these unique characteristics, biosensors based on peptides functionalized graphene have been effectively applied for drug or gene delivery (Tian et al., 2016) and detection of various analytes, including pollutants (Zhang et al., 2015b), proteins (Chiu et al., 2019), antibodies (Lu et al., 2011; Wu et al., 2014), proteases (Li et al., 2019; Yang et al., 2016), and pathogens (Chen and Nugen, 2019; Lim et al., 2015), etc. In the following, we lay emphasis on the designing and application of peptides-graphene biosensors for bacterial and viral pathogens detection, and a summary of relevant researches is listed in Table 4. Besides, the antibacterial effect and mechanism of antibacterial peptide-graphene complexes are also discussed.

In order to enhance the sensitivity of the peptide-graphene biosensor, as many peptide probe molecules as possible should be modified on the surface of graphene. Given the simplicity and non-destructivity (have no effect on the structure and properties of nanomaterials and peptides), non-covalent conjugation strategy that mediated by physical effects (e.g. π–π stacking, electrostatic force, hydrophobic interaction, etc.) still occupies an important position in the preparation of peptide-graphene biosensors (Lim et al., 2015). Besides, due to the flexibility of peptide sequence designing, a more stable modification effect can be achieved by selecting a specific amino sequence with a stronger affinity to the graphene surface. It has been demonstrated that the adsorption strength of amino acids on the GO surface followed the order of arginine (Arg) > histidine (His) > lysine (Lys) > tryptophan (Trp) > tyrosine (Tyr) > phenylalanine (Phe) (Zhang et al., 2011). On the other hand, ENC/NHS chemical coupling is also a prevalent method for the construction of peptide-graphene biosensors, in which the amino groups on the peptide molecules react with the carboxyl groups on the graphene surface (Yuan et al., 2018). Whereas, because of the limited number of carboxyl groups on graphene, the introduction of pyrene- or porphyrin-based bifunctional crosslinkers provides an effective path to increase the loading of peptide on graphene (Chan et al., 2015).

Generally, the design of peptides-graphene-based biosensors for target detection mainly relies on two principles. The first is that the cleavage of specific peptide chains by targets results in the change of signals. For instance, Zhang et al. reported a sensitive fluorescence biosensing platform constructed by covalently binding FAM-labeled peptide molecules to the surface of GO (Zhang et al., 2018). In the presence of HIV-1 protease, the FAM-labeled substrate peptides were cleaved into short fragments, thus regaining the fluorescence quenched by GO (Fig. 7A). This sensing strategy showed accurate and sensitive

Table 4
Peptide-graphene biosensors for detecting pathogens.

Peptide sequence	Biosensor design	Interactions	Target	Biosensor type	Linear range	LOD	Ref.
SNAP-25 peptide	rGO	Pyrenebutyric acid linker	Botulinum neurotoxin A (BoNT/A) enzymatic activity	Electrochemistry	1 pg/mL–1 ng/mL	8.6 pg/mL	Chan et al. (2015)
GIGKFLHSAGKFGKAFVGEIMKS	holey rGO	EDC/NHS	*E. coli* O157:H7	Electrochemistry	10^4–10^7 CFU/mL	803 CFU/mL	Chen et al. (2014)
KKNYSSSISSIHC	AgNPs-GO	Electrostatic interaction	LPS	Electrochemistry	0.0005–1 EU/mL	0.001 EU/mL	Yu et al. (2019)
KKNYSSSISSIHC	GO	Electrostatic interactions and/or π–π stacking	LPS	Fluorescence	2 nM–10 μM	130 pM	Lim et al. (2015)
RKRFRENLYFQSCP	GO	Electrostatic interaction	Tobacco etch virus (TEV) protease and engineered phage-infected bacteria	Fluorescence	TEV protease: 0–0.4 μg/μL bacteria: 10^3–10^7 CFU/mL	TEV protease: 51 ng/μL bacteria:10^4 CFU/mL	Chen and Nugen (2019)
SNAP-25 peptide	GO	EDC/NHS	Botulinum neurotoxin A (BoNT/A) enzymatic activity	Fluorescence	1 fg/mL–1 pg/mL	1 fg/mL	Shi et al. (2015)
RKRIHIGPGPAFYTT	GO	π–π stacking and hydrophobic interactions	HIV antibody	Fluorescence	5–150 nM	2 nM	Wu et al. (2014)
CALNNSQNYPIVQK	GO	EDC/NHS	HIV-1 protease	Fluorescence	5–300 ng/mL	1.18 ng/mL	Zhang et al. (2018)
RS5: RYWMS; QY7: QGYGYNY; ED17: EINPDSSTINYTPSLKD	GO	π–π stacking	Ebola virus (EBOV), Marburg virus (MARV), and Vesicular Stomatitis virus (VSV)	Fluorescence	EBOV: 0–15 ng/mL; MARV: 0–15 ng/mL; SV: 0–15 ng/mL	–	Fu et al. (2020)
GIGKFLHSAGKFGKAFVGEIMKS	AgNPs-rGO	Au–S bond	*E. coli* O157:H7	Surface plasmon resonance	1.0×10^3–5.0×10^7 CFU/mL	5.0×10^2 CFU/mL	Zhou et al. (2018b)
Bacitracin A	Au@Ag-GO	EDC/NHS	*E. coli*, *S. aureus* and *P. aeruginosa*	Surface-enhanced Raman scattering	10^1–10^6 CFU/mL	10^1 CFU/mL	Yuan et al. (2018)

detection for HIV-1 protease and exhibited successful application for detection of HIV-1 protease in human serum. Based on a similar principle, Chan and colleagues fabricated an ultrasensitive electrochemical biosensor for the detection of botulinum neurotoxin serotype A light chain (BoNT-LcA) protease activity with a low LOD around 5 pg/mL (Chan et al., 2015). The presence of BoNT-LcA could specifically shear the cleavage sites of SNAP-25-GFP, releasing the cleaved fragments from the electrode surface, which could be monitored by DPV due to the reduction of electrostatic repulsion and steric hindrance.

The second strategy is based on the separation of peptide chains from graphene surface or the attachment of analytes on peptides-graphene complexes as a result of the potent force between the peptide and target. In recent, Yu et al. designed a sensitive electrochemical biosensor that used peptides as specific recognition elements while GO and ferrocene-DNA-modified gold nanoparticles as electrochemical signal transducers for the determination of endotoxin (Yu et al., 2019). In the absence of endotoxin, the Fc-DNA-AuNPs complexes allowed to be attached on the peptides/GO/electrode surface due to the Au–S chemistry between AuNPs and the cysteine thiol group labeled at the terminal of the peptide, so that an obvious Fc response could be exhibited. Nevertheless, with the addition of endotoxin, the peptides were desorbed from GO because of the interaction with targets. Consequently,the AuNPs with negative charges could not be facilely anchored to the electrode, and reducing the electrochemical signal (Fig. 7B).

As part of the innate immune system of many organisms, antimicrobial peptides (AMPs) play an essential role in protecting against microbial invasion, including viruses, bacteria, and fungi (Nguyen et al., 2011). AMPs, a class of cationic and amphiphilic short-peptide, could bind to the surface of microbial cells via electrostatic interactions with LPS or other negatively-charged molecules on bacterial membranes, and present their antibacterial ability through membrane destruction (Brogden, 2005). Based on the recognition of phosphate groups on LPS by AMPs, numerous biosensors using AMPs as recognition molecules have been developed for the detection, classification and quantification of bacteria and viruses (Pavan and Berti, 2012). The first biosensor utilizing AMP to capture target was reported by Nadezhda V. Kulagina and co-workers, which was an array-based biosensor applying the AMP Magainin I to detect *E. coli* O157: H7 and *S. Typhimurium* (Kulagina et al., 2005). Specifically, under the assisted signal amplification effect of graphene materials, it has been turned out that the AMPs-Graphene biosensors have a potential application for the sensitive determination and accurate classification of pathogens.

According to Chen's report, a FET biosensor was constructed by covalently immobilizing Magainin I on the surface of holey reduced graphene oxide (hRGO) for the determination of gram-negative bacteria, which could convert the interaction between Magainin I and *E. coli* O157: H7 into conductance changes (Chen et al., 2014). By comparison with other related carbon nanomaterials, hRGO-FET devices exhibited a superior detection performance since hRGO retained the essential electronic properties and provided the abundant oxygen-containing groups required for covalent modification. Likewise, Zhou et al. applied Magainin I to fabricate a fiber optical surface plasmon resonance

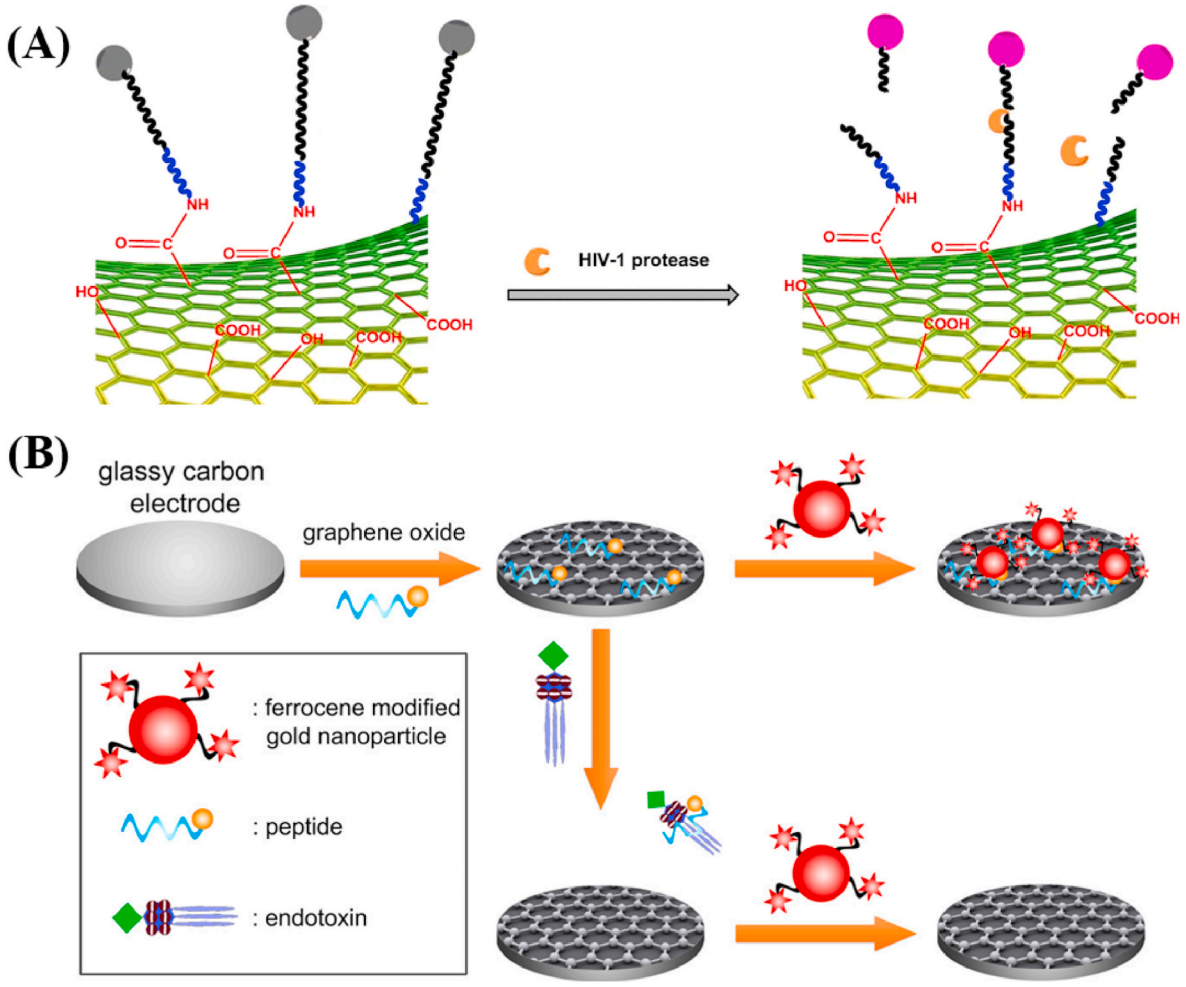

Fig. 7. (A) The detection principle based on the cleavage of specific peptide chains by targets. (Reproduced with permission from Ref. (Zhang et al., 2018). Copyright 2018, Springer). (B) Strategy based on the separation of peptide chains from graphene materials surface due to the binding of targets and peptides. (Reproduced with permission from Ref. (Yu et al., 2019). Copyright 2019, American Chemical Society).

(FOSPR) biosensor for *E. coli* O157: H7 detection, where AgNPs-rGO served as a signal transduction and amplification element (Fig. 8A) (Zhou et al., 2018). With the specific capture of *E. coli* O157: H7 by Magainin I-AgNPs-rGO coated FOSPR probes, the refractive index of optical fiber surface was altered gradually, thereby resulting in the shift of surface plasma absorption peak wavelength. The sensitive detection performance (LOD: 5×10^2 CFU/mL) of this assay demonstrated the feasibility of detecting *E. coli* O157: H7 in uncultured food samples directly and rapidly.

It is essential to discriminate various bacteria for the rapid elimination of infections in clinical application, and plenty of methods on the classification of bacteria have been proposed. Lately, a facile method to classify clinic isolates with a turn-off sensor array based on GO and AMPs was established by Fan and colleagues (Fan et al., 2020). In this study, two typical AMPs, including Ib-AMP4 and thanatin, which have excellent targeting capability against gram-positive and gram-negative bacteria respectively, were fused by the poly-histidine adaptor that can bind to GO for constructing the AMPs-poly-histidine-FAM peptides (Fig. 8B). Due to the opposite targeting and binding preferences of Ib-AMP4 and thanatin, they exhibited different affinity to diverse bacterial species, thus presenting related fluorescence signals and allowing a good resolution of bacterial species. Thirteen kinds of the most common clinical bacterial species were examined and the obtained fluorescent intensities were used for discrimination of bacteria via stepwise linear discriminant analysis (LDA), so that the training matrix was established successfully. After verification of the collected 155 clinical isolates, the sensor array revealed an excellent resolution and high accuracy, which is significant for clinical applications.

Apart from the ability to recognize and distinguish different species of bacteria, AMPs have a vitally important function of inhibiting or even killing bacteria, viruses, cancer cells, etc. There are two main direct-action mechanisms of AMPs on pathogens, including membrane permeabilizing and non-membrane targeting (Ulm et al., 2012). The membrane targeting AMPs interact with specific membrane receptors or cell membrane components through electrostatic and hydrophobic interactions to accumulate on the membrane surface and self-assemble after reaching a certain concentration (Andersson et al., 2016). After that, a transmembrane ion channel is formed on the membrane, which destroys the integrity of the membrane and induces the leakage of intracellular materials, resulting in cell death. Whereas, the non-membrane targeted AMPs bind with various precursor molecules required for cell wall synthesis to inhibit the synthesis of cell walls (Kumar et al., 2018), or combine with intracellular targets (proteins, nucleic acids, enzymes, etc.) to block key cellular processes such as inhibiting protein/nucleic acid synthesis and disrupting enzyme/protein activity (Brogden, 2005).

However, AMPs are still challenging to put into clinical practice due to their low cell penetration efficiency, high costs and cytotoxicity, and ease of enzymatic hydrolysis (Lázár et al., 2018). Therefore, modification of AMPs with nanomaterials that can spontaneously penetrate cell membranes and protect AMPs from enzymatic hydrolysis is a promising solution. Graphene materials, especially graphene or GO nanosheets, can be inserted into the membrane through their sharp edges and corners, resulting in increased membrane stress or intracellular material leakage to achieve the antibacterial effects (Li et al., 2013b), which are ideal materials to integrate with AMPs for an enhanced antibacterial activity. Lu and colleagues designed a hybrid compound of AMP melittin and graphene/GO nanosheets to achieve a preferable antibacterial effect, which showed significant efficiency in transmembrane perforation compared with the original melittin and hoisted the antibacterial capacity against Gram-positive and Gram-negative bacteria by 20 times (Lu et al., 2019). Ren et al. synthesized an AMP-grafted GO nanosheets complex, i.e., D28@GO, which possessed a strong effect on inhibiting the growth of pathogens such as *C. Albicans* and *E. coli* etc., and suppressed systemic infection of *C. Albicans* in vivo remarkably (Ren et al., 2019). This inhibitory mechanism may be relevant to membrane injury as a result of the interaction between D28@GO and biomacromolecules such as phospholipid and polysaccharides. In addition, several reports have demonstrated the application of AMPs-conjugated GO membranes to effectively remove and kill pathogenic bacteria, which is of great significance for the separation and elimination of pathogens in water (Kanchanapally et al., 2015; Viraka Nellore et al., 2015).

4.4. Other biomolecules-functionalized graphene biosensors

Other biomolecules, such as bacteriophages, antigens, the whole cells, lectins, glycans, have also been used for the functionalization of graphene nanomaterials to recognize pathogenic microorganisms. Bacteriophage is a class of viruses that can specifically infect and invade the target bacteria's cellular mechanism to hasten its own growth and multiply, and is prevalent in the soils, foods and surface water. Bacteriophages typically make use of their tail proteins to perform specific

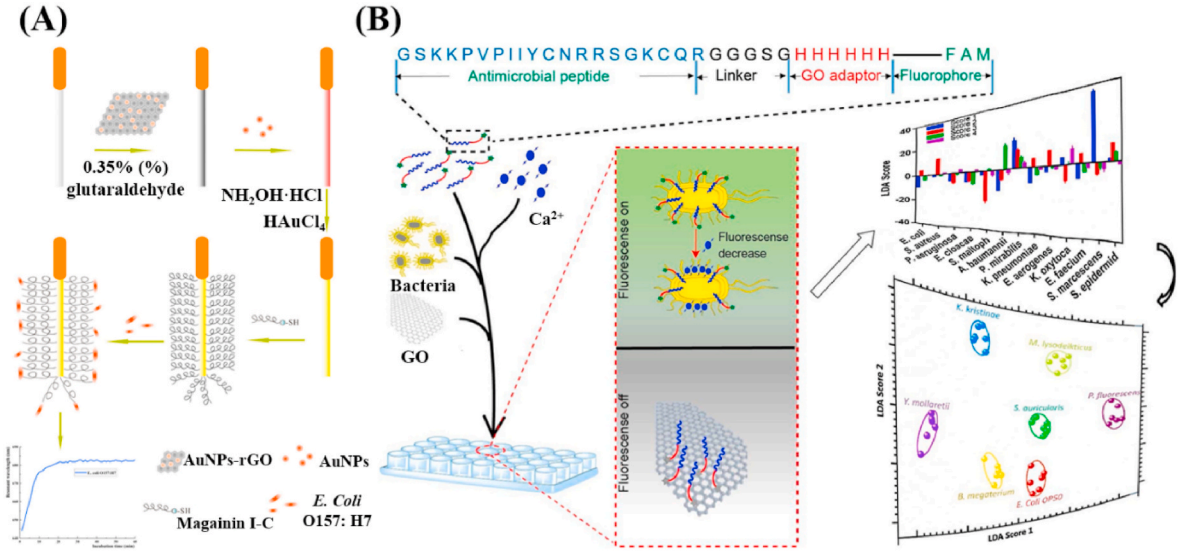

Fig. 8. (A) Schematic diagram of the preparation of Magainin I-AgNPs-rGO coated FOSPR probes and detection of *E. coli* O157: H7. (Reproduced with permission from Ref. (Zhou et al., 2018). Copyright 2018, Elsevier). (B) The design principle of the sensor array based on GO and AMP to classify diverse clinic isolates. (Reproduced with permission from Ref. (Fan et al., 2020). Copyright 2020, Elsevier).

recognition and binding of host bacterial receptors at the level of the strain. And then the DNA in their heads are injected into the host cytoplasm by diffusion, permeation pressure, or specific protein transport, thereby utilizing the replication mechanisms of the host cell to assemble offspring bacteriophages (Grayson and Molineux, 2007). Based on the above characteristics, bacteriophages are regarded as an important biorecognition element for the development of highly specific bacterial biosensors, and have the additional advantages of distinguishing living cells from dead cells, no sample pretreatment and self-amplification requirement, as well as low cost of equipment production (Hagens and Loessner, 2007).

Bhardwaj et al. first proposed the application of bacteriophage electrochemical biosensors in the detection of *Staphylococcus arlettae* with high sensitivity and selective impedance measurements by attaching bacteriophages to graphene electrodes (Bhardwaj et al., 2016). This strategy was capable of detecting low concentrations of bacteria with a LOD of 2 CFU/mL, and allowed shorter response time than previous bacteria-lysis techniques because it directly recorded the signals produced by bacteria-bacteriophage binding. Similarly, a bacteriophage-modified GO screen-printed electrodes based impedimetric biosensor was proposed by Quiton and co-workers for the determination of *S. Typhimurium* (Quiton et al., 2018). Keihan et al. anchored bacteriophage on a carbon-paste electrode surface that was coated with reduced graphene to produce an unlabeled capacitive biosensor, so as to rapidly detect *E. coli* within about 5 s (Keihan et al., 2019).

The indirect quantitative analysis via immobilizing the detected targets onto the substrate is also a common method in biosensors, such as indirect assay in ELISA. Therefore, graphene biosensors modified with antigens, specific proteins and even whole cells have been developed to reflect the presence of bacteria and viruses indirectly. The production of anti-HBcAg antibodies against the Hepatitis B virus core antigen

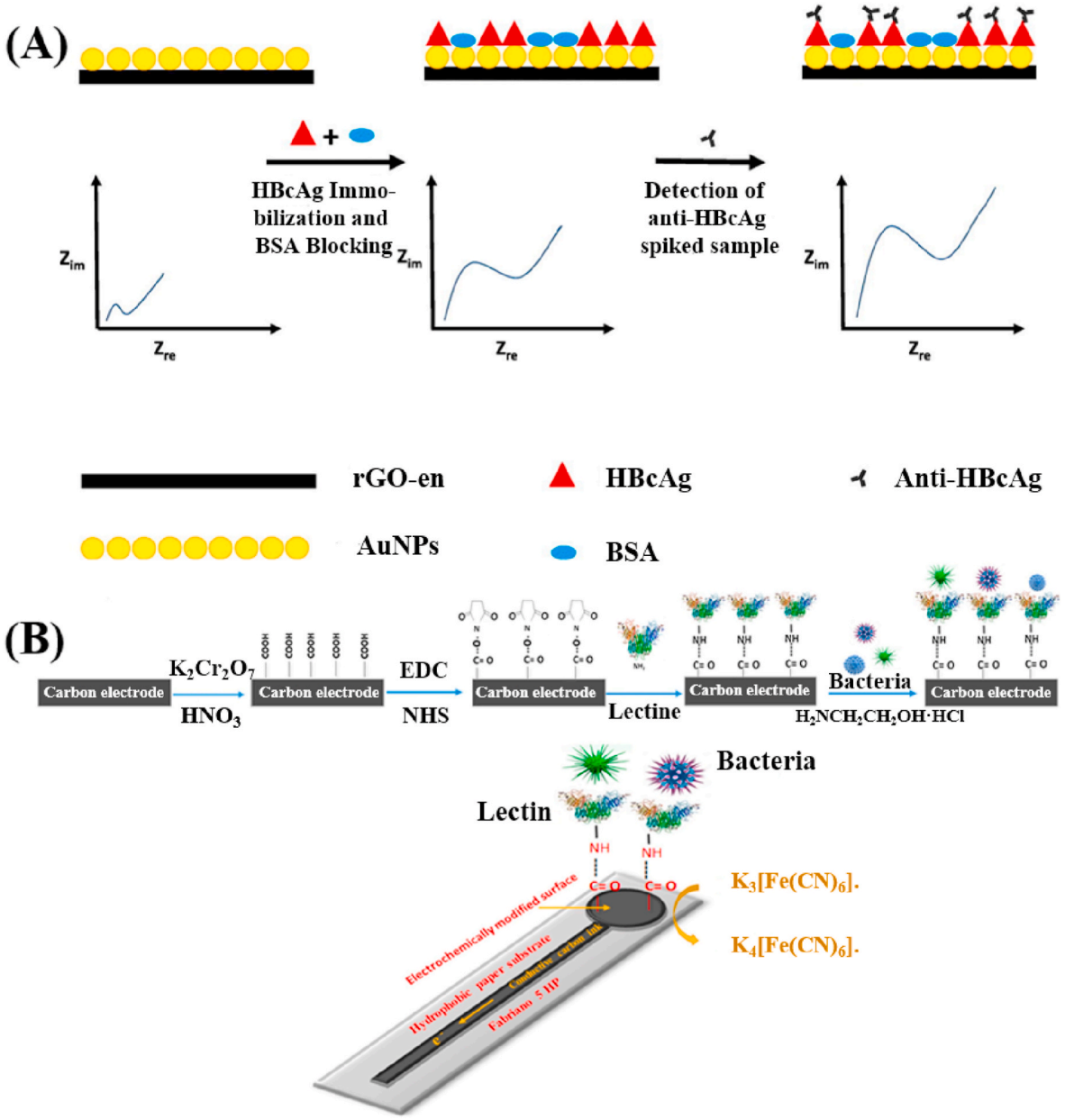

Fig. 9. (A)Designing of immobilizing HBcAg onto rGO-en-AuNPs nanocomposites surface to determine the presence of anti-HBcAg. (Reproduced with permission from Ref. (Muain et al., 2018). Copyright 2018, Elsevier). (B) Schematic diagram depicting the modification procedure of ConA lectin functionalized paper-based electrode and the principle of bacterial detection. (Reproduced with permission from Ref. (Rengaraj et al., 2018). Copyright 2018, Elsevier).

(HBcAg) in the serum indicates that the body has been infected by the Hepatitis B virus (HBV). Based on it, the HBcAg were immobilized on the surface of rGO-en-AuNPs nanocomposites to determine the presence of anti-HBcAg by impedance measurements, which could reflect whether a person was exposed to HBV, and could therefore potentially be used to screen anti-HBcAg blood before transfusions or organ transplants to healthy recipients (Fig. 9A) (Muain et al., 2018). Anik and co-workers prepared a sensitive electrochemical neuraminidase activity assay biosensor for the determination of real influenza A virus (H9N2) by immobilizing specific surface glycoprotein neuraminidase of influenza A virus on graphene-gold electrodes modified with fetoglobulin A (Anik et al., 2018). The terminal sialic acid residues in the fetuin A molecules were cleaved by neuraminidases, and then this process was monitored by adding peanut lectin on the electrode surface.

Lectins can also be served as biorecognition elements because it selectively interacts with carbohydrate molecules such as monosaccharides, oligosaccharides and glycoproteins on bacterial cells (Ertl and Mikkelsen, 2001; Sadik and Yan, 2007). Concanavalin A (ConA) is a common lectin that can specifically recognize both α-D-glucose and α-D-mannose groups on the surface of *E. coli*, *Bacillus sp.* and other bacteria (Gamella et al., 2009). Rengaraj et al. designed a ConA functionalized paper-based electrode for detecting bacteria in water, proving that ConA lectin is an effective recognition molecule (Fig. 9B) (Rengaraj et al., 2018). Qin and colleagues constructed an impedimetric biosensor utilizing AuNPs–Graphene electrode modified with ConA for the sensitive detection of LPS on the bacterial outer membrane with the detection limit of 600 pg/L (Qin et al., 2019). Moreover, glycans functionalized graphene-based biosensor has been reported for the diagnosing of human-infectious avian influenza virus infections (Ono et al., 2017). In a word, there are many biomolecules that can specifically identify bacteria or viruses and their biomarkers, which could achieve more accurate and sensitive detection of various bacterial and viral pathogens through combining with graphene materials, and we have reason to believe that more of these biomolecules will be discovered to promote the developments in the field of detection and elimination of pathogens.

5. Summary and outlook

In summary, graphene biosensors have opened up a new approach for the rapid and straightforward detection of pathogenic bacteria and viruses. In this review, we have mainly summed up the representative bio-functionalized graphene biosensors for the detection of bacterial and viral pathogens as well as their working mechanism. Also, the preparation, properties and bio-functionalization of graphene are briefly introduced. This work provides important guidance for broadening the application of graphene materials and developing new pathogenic detection strategies for the prevention and control of infectious diseases. Although graphene biosensors have extensive application prospects, some drawbacks should not be ignored. For instance, since graphene also has a certain adsorption capacity to non-target substances, false positive signals are likely to be generated if non-covalent functionalization methods are applied, while most covalent strategies are very complex and require precise conditional control. Besides, the affinity and load of graphene for biomolecules are easily affected by the external environment (temperature, pH, salt concentration, etc.) and their own properties (type and weight of biomolecules, surface properties of graphene, etc.). Therefore, in order to further improve their performance and efficiency, there are still some challenges that need to be noted.

Firstly, it is difficult to ensure the homogeneity of graphene in terms of size, thickness, biocompatibility and number of surface functional groups. Such inhomogeneity not only affects the surface functionalization efficiency of graphene, but also has a great impact on the performance evaluation and reproducibility of the constructed biosensors. Secondly, how to develop a bio-functionalization method that can maintain high stability without changing the structure and function of biomolecules and graphene materials is also a tough challenge. Finally, because of the complexity of the environment in which pathogens exist, it is essential to carry out pretreatment processes (purification and/or concentration) of samples to avoid interference from other substrates. Therefore, simplified and effective sample preparation methods should be further studied, which is significant for timely diagnosis and large-scale spread control in the early stage of pathogen infection. Despite the above challenges we still face, it is anticipated that these issues will be overcome and graphene biosensor system will be more sophisticated as further study continues.

So far, considering practical applications and mass production for epidemic prevention, more attention should be paying to miniaturized biofunctionalized graphene biosensors with the advantages of portability and time/cost savings, such as field-effect transistors, microfluidics chips and lateral-flow assay. Further, portable miniaturization devices that collect signals via smartphones and wireless transduction can provide an excellent convenience for field detection of pathogens in remote and wild areas. Besides, due to the diversity of pathogen species in the environment, multi-channel detection equipment capable of detecting multiple pathogens simultaneously without mutual interference is also the main development direction of biosensor design in the future. To some extent, the multiplex sensor designing has the potential to simplify the analysis procedure and improve the detection efficiency. Moreover, given the fact that graphene materials and certain biomolecules have the ability to resist and damage pathogens, we suppose that more biosensors that integrate the functions of detection and specific killing of target pathogens will be designed. This multi-functional graphene biosensor can not only broaden its application in other fields such as pathogen filtration of drinking water or air, but also effectively prevent secondary infection from discarded detection equipment. Last but not least, environmental friendliness and resource conservation have always been essential principles in sensor design, so that the harmlessization and reusability of detection devices should also be taken into account.

Declaration of competing interest

The authors declare that they have no known competing financial interests or personal relationships that could have appeared to influence the work reported in this paper.

Acknowledgments

This work was supported by the National Natural Science Foundation of China (grant no. 21777135, 51708475) and Hunan Provincial Natural Science Foundation (grant no. 2019JJ40283, 2019JJ50596, 2018JJ3496, 2019JJ30025), the Research Foundation of Education Bureau of Hunan Province (19A501, 18C0102), and Hunan 2011 Collaborative Innovation Center of Chemical Engineering & Technology with Environmental Benignity and Effective Resource Utilization.

References

Afsahi, S., Lerner, M.B., Goldstein, J.M., Lee, J., Tang, X., Bagarozzi Jr., D.A., Pan, D., Locascio, L., Walker, A., Barron, F., 2018. Biosens. Bioelectron. 100, 85–88.
Aguirre, S.D., Ali, M.M., Salena, B.J., Li, Y., 2013. Biomolecules 3, 563–577.
Ahmed, S.R., Takemeura, K., Li, T.C., Kitamoto, N., Tanaka, T., Suzuki, T., Park, E.Y., 2017. Biosens. Bioelectron. 87, 558–565.
Akcöltekin, S., El Kharrazi, M., Köhler, B., Lorke, A., Schleberger, M., 2009. Nanotechnology 20, 155601.
Akhavan, O., Ghaderi, E., Esfandiar, A., 2011. J. Phys. Chem. B 115, 6279–6288.
Ali, M.M., Aguirre, S.D., Lazim, H., Li, Y., 2011. Angew. Chem. Int. Ed. 50, 3751–3754.
Allen, M.J., Tung, V.C., Kaner, R.B., 2010. Chem. Rev. 110, 132–145.
Andersson, D.I., Hughes, D., Kubicek Sutherland, J.Z., 2016. Drug Resist. Updates 26, 43–57.
Anik, Ü., Tepeli, Y., Sayhi, M., Nsiri, J., Diouani, M.F., 2018. Analyst 143, 150–156.
Anju, M., Renuka, N., 2019. Nano Struct. Nano Objects 17, 194–217.
Ansari, N., Ghazvini, K., Ramezani, M., Shahdordizadeh, M., Yazdian Robati, R., Abnous, K., Taghdisi, S.M., 2018. Microchim. Acta 185, 21.
Appaturi, J.N., Pulingam, T., Thong, K.L., Muniandy, S., Ahmad, N., Leo, B.F., 2020. Anal. Biochem. 589, 113489.

Bahadır, E.B., Sezgintürk, M.K., 2016. TrAC Trends Anal. Chem. (Reference Ed.) 76, 1–14.
Ballantine Jr., D., White, R.M., Martin, S.J., Ricco, A.J., Zellers, E., Frye, G., Wohltjen, H., 1996. Acoustic Wave Sensors: Theory, Design and Physico-Chemical Applications. Elsevier.
Bhardwaj, N., Bhardwaj, S.K., Mehta, J., Mohanta, G.C., Deep, A., 2016. Anal. Biochem. 505, 18–25.
Bolotin, K.I., Sikes, K.J., Jiang, Z., Klima, M., Fudenberg, G., Hone, J., Kim, P., Stormer, H., 2008. Solid State Commun. 146, 351–355.
Brogden, K.A., 2005. Nat. Rev. Microbiol. 3, 238–250.
Bu, T., Wang, J., Huang, L., Dou, L., Zhao, B., Li, T., Zhang, D., 2019. J. Agric. Food Chem. 67, 6642–6649.
Chan, C.Y., Guo, J., Sun, C., Tsang, M.K., Tian, F., Hao, J., Chen, S., Yang, M., 2015. Sensor. Actuator. B Chem. 220, 131–137.
Chan, C., Shi, J., Fan, Y., Yang, M., 2017. Sensor. Actuator. B Chem. 251, 927–933.
Chand, R., Neethirajan, S., 2017. Biosens. Bioelectron. 98, 47–53.
Cheeveewattanagul, N., Morales Narváez, E., Hassan, A.R.H., Bergua, J.F., Surareungchai, W., Somasundrum, M., Merkoçi, A., 2017. Adv. Funct. Mater. 27, 1702741.
Chekin, F., Bagga, K., Subramanian, P., Jijie, R., Singh, S.K., Kurungot, S., Boukherroub, R., Szunerits, S., 2018. Sensor. Actuator. B Chem. 262, 991–1000.
Chen, J., Nugen, S.R., 2019. Anal. Bioanal. Chem. 411, 2487–2492.
Chen, Y., Li, Y., Yang, Y., Wu, F., Cao, J., Bai, L., 2017. Microchim. Acta 184, 1801–1808.
Chen, Y., Michael, Z.P., Kotchey, G.P., Zhao, Y., Star, A., 2014. ACS Appl. Mater. Interfaces 6, 3805–3810.
Chinnappan, R., AlAmer, S., Eissa, S., Rahamn, A.A., Salah, K.M.A., Zourob, M., 2018. Microchim. Acta 185, 61.
Chiu, N.F., Kuo, C.T., Chen, C.Y., 2019. Int. J. Nanomed. 14, 4833.
Chiu, N.F., Kuo, C.T., Lin, T.L., Chang, C.C., Chen, C.Y., 2017. Biosens. Bioelectron. 94, 351–357.
Choi, J.R., 2020. Front. Chem. 8, 517.
Choi, J.R., Hu, J., Tang, R., Gong, Y., Feng, S., Ren, H., Wen, T., Li, X., Abas, W.A.B.W., Pingguan Murphy, B., 2016. Lab Chip 16, 611–621.
Choi, J.R., Tang, R., Wang, S., Abas, W.A.B.W., Pingguan Murphy, B., Xu, F., 2015. Biosens. Bioelectron. 74, 427–439.
Dai, G., Li, Z., Luo, F., Ai, S., Chen, B., Wang, Q., 2019. Microchim. Acta 186, 620.
Donskyi, I.S., Azab, W., Cuellar Camacho, J.L., Guday, G., Lippitz, A., Unger, W.E., Osterrieder, K., Adeli, M., Haag, R., 2019. Nanoscale 11, 15804–15809.
Dowaidar, M., Abdelhamid, H.N., Hällbrink, M., Zou, X., Langel, Ü., 2017. Biochim. Biophys. Acta Gen. Subj. 1861, 2334–2341.
Du, T., Lu, J., Liu, L., Dong, N., Fang, L., Xiao, S., Han, H., 2018. ACS Appl. Biol. Mater. 1, 1286–1293.
Duan, N., Shen, M., Wu, S., Zhao, C., Ma, X., Wang, Z., 2017. Microchim. Acta 184, 2653–2660.
Dye, C., 2014. Philos. Trans. Roy. Soc. B. Biol. Sci. 369, 20130426.
Egholm, M., Buchardt, O., Christensen, L., Behrens, C., Freier, S.M., Driver, D.A., Berg, R. H., Kim, S.K., Norden, B., Nielsen, P.E., 1993. Nature 365, 566–568.
Ertl, P., Mikkelsen, S.R., 2001. Anal. Chem. 73, 4241–4248.
Fan, X., Xu, W., Gao, W., Jiang, X., Wu, G., 2020. Sensor. Actuator. B Chem. 307, 127607.
Farzin, L., Sadjadi, S., Shamsipur, M., Sheibani, S., 2020. J. Pharmaceut. Biomed. Anal. 179, 112989.
Fei, J., Dou, W., Zhao, G., 2016. Microchim. Acta 183, 757–764.
Fu, M.Q., Wang, X.C., Dou, W.T., Chen, G.-R., James, T.D., Zhou, D.M., He, X.P., 2020. Chem. Commun.
Gamella, M., Campuzano, S., Parrado, C., Reviejo, A., Pingarrón, J., 2009. Talanta 78, 1303–1309.
Gong, Q., Han, H., Yang, H., Zhang, M., Sun, X., Liang, Y., Liu, Z., Zhang, W., Qiao, J., 2019. J. Materiom. 5, 313–319.
Gong, Q., Wang, Y., Yang, H., 2017. Biosens. Bioelectron. 89, 565–569.
Grayson, P., Molineux, I.J., 2007. Curr. Opin. Microbiol. 10, 401–409.
Gupta, A., Bhardwaj, S.K., Sharma, A.L., Deep, A., 2019. Microchim. Acta 186, 800.
Gurunathan, S., Han, J.W., Dayem, A.A., Eppakayala, V., Kim, J.H., 2012. Int. J. Nanomed. 7, 5901.
Hagens, S., Loessner, M.J., 2007. Appl. Microbiol. Biotechnol. 76, 513–519.
He, J., Zhu, X., Qi, Z., Wang, C., Mao, X., Zhu, C., He, Z., Li, M., Tang, Z., 2015. ACS Appl. Mater. Interfaces 7, 5605–5611.
Hernández, R., Vallés, C., Benito, A.M., Maser, W.K., Rius, F.X., Riu, J., 2014. Biosens. Bioelectron. 54, 553–557.
Hoyos Nogués, M., Gil, F., Mas Moruno, C., 2018. Molecules 23, 1683.
Hu, W., Peng, C., Luo, W., Lu, M., Li, X., Li, D., Huang, Q., Fan, C., 2010. ACS Nano 4, 4317–4323.
Hu, W., Peng, C., Lu, M., Li, X., Zhang, Y., Chen, N., Fan, C., Huang, Q., 2011. ACS Nano 5, 3693–3700.
Hu, Y., Zhang, Q., Guo, Z., Wang, S., Du, C., Zhai, C., 2017. Biosens. Bioelectron. 98, 91–99.
Hu, Y., Zhang, Q., Hu, D., Wang, J., Rao, J., Xu, L., Guo, Z., Wang, S., Liu, X., Tang, S., 2019. Microchim. Acta 186, 325.
Huang, H., Bai, W., Dong, C., Guo, R., Liu, Z., 2015. Biosens. Bioelectron. 68, 442–446.
Huang, J., Xie, Z., Xie, Z., Luo, S., Xie, L., Huang, L., Fan, Q., Zhang, Y., Wang, S., Zeng, T., 2016. Anal. Chim. Acta 913, 121–127.
Huang, Y., Sutter, E., Shi, N.N., Zheng, J., Yang, T., Englund, D., Gao, H.J., Sutter, P., 2015b. ACS Nano 9, 10612–10620.
Iliuk, A.B., Hu, L., Tao, W.A., 2011. Anal. Chem. 83, 4440–4452.
Innocenzi, P., Stagi, L., 2020. Chem. Sci.
Islam, S., Shukla, S., Bajpai, V.K., Han, Y.K., Huh, Y.S., Kumar, A., Ghosh, A., Gandhi, S., 2019. Biosens. Bioelectron. 126, 792–799.
Jaiswal, N., Pandey, C.M., Solanki, S., Tiwari, I., Malhotra, B.D., 2020. Microchim. Acta 187, 1.
Jeong, S., Kim, D.M., An, S.Y., Kim, D.H., Kim, D.E., 2018. Anal. Biochem. 561, 66–69.
Ji, H., Sun, H., Qu, X., 2016. Adv. Drug Deliv. Rev. 105, 176–189.
Ji, J., Pang, Y., Li, D., Wang, X., Xu, Y., Mu, X., 2020. ACS Appl. Mater. Interfaces 12, 12417–12425.
Jia, F., Duan, N., Wu, S., Dai, R., Wang, Z., Li, X., 2016. Microchim. Acta 183, 337–344.
Jijie, R., Kahlouche, K., Barras, A., Yamakawa, N., Bouckaert, J., Gharbi, T., Szunerits, S., Boukherroub, R., 2018. Sensor. Actuator. B Chem. 260, 255–263.
Jin, X., Zhang, H., Li, Y.T., Xiao, M.M., Zhang, Z.L., Pang, D.W., Wong, G., Zhang, Z.Y., Zhang, G.J., 2019. Microchim. Acta 186, 223.
Justino, C.I., Duarte, A.C., Rocha Santos, T.A., 2016. TrAC Trends Anal. Chem. (Reference Ed.) 85, 36–60.
Justino, C.I., Gomes, A.R., Freitas, A.C., Duarte, A.C., Rocha Santos, T.A., 2017. TrAC Trends Anal. Chem. (Reference Ed.) 91, 53–66.
Kanchanapally, R., Nellore, B.P.V., Sinha, S.S., Pedraza, F., Jones, S.J., Pramanik, A., Chavva, S.R., Tchounwou, C., Shi, Y., Vangara, A., 2015. RSC Adv. 5, 18881–18887.
Kaur, H., Shorie, M., Sharma, M., Ganguli, A.K., Sabherwal, P., 2017. Biosens. Bioelectron. 98, 486–493.
Keihan, A.H., Hosseinzadeh, G., Sajjadi, S., Ashiani, D., Dashtestani, F., Eskandari, K., 2019. Nanosci. Nanotechnol. - Asia 9, 408–413.
Kim, S., Ryoo, S.R., Na, H.K., Kim, Y.K., Choi, B.S., Lee, Y., Kim, D.E., Min, D.H., 2013. Chem. Commun. 49, 8241–8243.
Klein, D., 2002. Trends Mol. Med. 8, 257–260.
Kulagina, N.V., Lassman, M.E., Ligler, F.S., Taitt, C.R., 2005. Anal. Chem. 77, 6504–6508.
Kumar, P., Kizhakkedathu, J.N., Straus, S.K., 2018. Biomolecules 8, 4.
Lázár, V., Martins, A., Spohn, R., Daruka, L., Grézal, G., Fekete, G., Számel, M., Jangir, P. K., Kintses, B., Csörgő, B., 2018. Nat. Microbiol. 3, 718–731.
Law, J.W.F., Ab Mutalib, N.S., Chan, K.G., Lee, L.H., 2015. Front. Microbiol. 5, 770.
Lee, C.Y., Jang, H., Kim, H., Jung, Y., Park, K.S., Park, H.G., 2019. Microchim. Acta 186, 330.
Lee, J., Takemura, K., Kato, C.N., Suzuki, T., Park, E.Y., 2017. ACS Appl. Mater. Interfaces 9, 27298–27304.
Leonard, P., Hearty, S., Brennan, J., Dunne, L., Quinn, J., Chakraborty, T., O'Kennedy, R., 2003. Enzym. Microb. Technol. 32, 3–13.
Li, J., Li, Y., Zhai, X., Cao, Y., Zhao, J., Tang, Y., Han, K., 2020a. Electrochem. Commun. 110, 106601.
Li, P., Chen, X., Yang, W., 2013a. Langmuir 29, 8629–8635.
Li, Q., Wang, Y., Yu, G., Liu, Y., Tang, K., Ding, C., Chen, H., Yu, S., 2019. Nanoscale 11, 20903–20909.
Li, X., Wang, Y., Zhang, X., Gao, Y., Sun, C., Ding, Y., Feng, F., Jin, W., Yang, G., 2020b. Microchim. Acta 187, 1–9.
Li, Y., Luo, G., Qing, Z., Li, X., Zou, Z., Yang, R., 2019b. Microchim. Acta 186, 565.
Li, Y., Yuan, H., Von Dem Bussche, A., Creighton, M., Hurt, R.H., Kane, A.B., Gao, H., 2013b. Proc. Natl. Acad. Sci. U. S. A. 110, 12295–12300.
Lim, S.K., Chen, P., Lee, F.L., Moochhala, S., Liedberg, B., 2015. Anal. Chem. 87, 9408–9412.
Ling, S., Li, C., Adamcik, J., Wang, S., Shao, Z., Chen, X., Mezzenga, R., 2014. ACS Macro Lett. 3, 146–152.
Ling, X., Xie, L., Fang, Y., Xu, H., Zhang, H., Kong, J., Dresselhaus, M.S., Zhang, J., Liu, Z., 2010. Nano Lett. 10, 553–561.
Liu, J., Liu, Z., Barrow, C.J., Yang, W., 2015. Anal. Chim. Acta 859, 1–19.
Liu, M., Zhang, Q., Brennan, J.D., Li, Y., 2018b. MRS Commun. 8, 687–694.
Liu, M., Zhao, H., Chen, S., Yu, H., Quan, X., 2012a. Chem. Commun. 48, 564–566.
Liu, M., Zheng, C., Cui, M., Zhang, X., Yang, D.P., Wang, X., Cui, D., 2018c. Microchim. Acta 185, 458.
Liu, R., Wu, D., Feng, X., Müllen, K., 2011. J. Am. Chem. Soc. 133, 15221–15223.
Liu, Y., Dong, X., Chen, P., 2012b. Chem. Soc. Rev. 41, 2283–2307.
Lu, C.H., Li, J., Zhang, X.L., Zheng, A.X., Yang, H.H., Chen, X., Chen, G.N., 2011. Anal. Chem. 83, 7276–7282.
Lu, F., Zhang, S., Gao, H., Jia, H., Zheng, L., 2012. ACS Appl. Mater. Interfaces 4, 3278–3284.
Lu, X., Liu, J., Gou, L., Li, J., Yuan, B., Yang, K., Ma, Y., 2019. Adv. Healthc. Mater. 8, 1801521.
McConnell, E.M., Morrison, D., Rincon, M.A.R., Salena, B.J., Li, Y., 2019. TrAC Trends Anal. Chem. (Reference Ed.) 115785.
Meng, F., Sun, H., Huang, Y., Tang, Y., Chen, Q., Miao, P., 2019. Anal. Chim. Acta 1047, 45–51.
Mogha, N.K., Sahu, V., Sharma, R.K., Masram, D.T., 2018. J. Mater. Chem. B 6, 5181–5187.
Muain, M.F.A., Cheo, K.H., Omar, M.N., Hamzah, A.S.A., Lim, H.N., Salleh, A.B., Tan, W. S., Tajudin, A.A., 2018. Bioelectrochemistry 122, 199–205.
Muniandy, S., Dinshaw, I.J., Teh, S.J., Lai, C.W., Ibrahim, F., Thong, K.L., Leo, B.F., 2017. Anal. Bioanal. Chem. 409, 6893–6905.
Navakul, K., Warakulwit, C., Yenchitsomanus, P.T., Panya, A., Lieberzeit, P.A., Sangma, C., 2017. Nanomed. Nanotechnol. Biol. Med. 13, 549–557.
Nguyen, L.T., Haney, E.F., Vogel, H.J., 2011. Trends Biotechnol. 29, 464–472.
Ning, Y., Zou, L., Gao, Q., Hu, J., Lu, F., 2018. Microchim. Acta 185, 183.
Niu, J., Hu, X., Ouyang, W., Chen, Y., Liu, S., Han, J., Liu, L., 2018a. Anal. Chem. 91, 2360–2367.
Niu, X., Chen, W., Wang, X., Men, Y., Wang, Q., Sun, W., Li, G., 2018b. Microchim. Acta 185, 167.

Omar, N.A.S., Fen, Y.W., Abdullah, J., Zaid, M.H.M., Daniyal, W.M.E.M.M., Mahdi, M.A., 2019. Optic Laser. Technol. 114, 204–208.
Ono, T., Oe, T., Kanai, Y., Ikuta, T., Ohno, Y., Maehashi, K., Inoue, K., Watanabe, Y., Nakakita, S.i., Suzuki, Y., 2017. Jpn. J. Appl. Phys. 56, 030302.
Palmieri, V., Papi, M., 2020. Nano Today 100883.
Pandey, A., Gurbuz, Y., Ozguz, V., Niazi, J.H., Qureshi, A., 2017a. Biosens. Bioelectron. 91, 225–231.
Pandey, C.M., Tiwari, I., Singh, V.N., Sood, K., Sumana, G., Malhotra, B.D., 2017b. Sensor. Actuator. B Chem. 238, 1060–1069.
Park, K.S., Lee, C.Y., Park, H.G., 2015. Chem. Commun. 51, 9942–9945.
Patil, P.O., Pandey, G.R., Patil, A.G., Borse, V.B., Deshmukh, P.K., Patil, D.R., Tade, R.S., Nangare, S.N., Khan, Z.G., Patil, A.M., 2019. Biosens. Bioelectron. 111324.
Pavan, S., Berti, F., 2012. Anal. Bioanal. Chem. 402, 3055–3070.
Pinto, A.M., Goncalves, I.C., Magalhães, F.D., 2013. Colloids Surf. B Biointerfaces 111, 188–202.
Pokhrel, R., Bhattarai, N., Johnson, K.A., Gerstman, B.S., Stahelin, R.V., Chapagain, P.P., 2017. Biochem. Biophys. Res. Commun. 493, 176–181.
Pourmadadi, M., Shayeh, J.S., Omidi, M., Yazdian, F., Alebouyeh, M., Tayebi, L., 2019. Microchim. Acta 186, 787.
Pumera, M., Ambrosi, A., Bonanni, A., Chng, E.L.K., Poh, H.L., 2010. TrAC Trends Anal. Chem. (Reference Ed.) 29, 954–965.
Qin, J., Sun, H., Hao, H., Jia, L., Yao, C., Wang, Q., Yang, H., 2019. Sensor. Mater. 31, 2917–2929.
Qing, Z., Bai, A., Chen, L., Xing, S., Zou, Z., Lei, Y., Li, J., Liu, J., Yang, R., 2020a. CCS Chemistry, pp. 1–32.
Qing, Z., Bai, A., Xing, S., Zou, Z., He, X., Wang, K., Yang, R., 2019a. Biosens. Bioelectron. 137, 96–109.
Qing, Z., Hu, J., Xu, J., Lei, Y., Qing, T., Yang, R.H., 2020b. Chem. Sci. 11, 1985–1990.
Qing, Z., Luo, G., Xing, S., Zou, Z., Lei, Y., Liu, J., Yang, R., 2020c. Angew. Chem. Int. Ed.
Qing, Z., Xu, J., Hu, J., Zheng, J., He, L., Zou, Z., Yang, S., Tan, W., Yang, R., 2019b. Angew. Chem. Int. Ed. 58, 11574–11585.
Quinton, J., Kolodych, S., Chaumonet, M., Bevilacqua, V., Nevers, M.C., Volland, H., Gabillet, S., Thuéry, P., Créminon, C., Taran, F., 2012. Angew. Chem. Int. Ed. 51, 6144–6148.
Quiton, P.A., Carreon, B.M., Cruz Papa, D.M.D., Bergantin Jr., J., 2018. Sens. Transducers J. 28, 38–42.
Ray, A., Nordén, B., 2000. Faseb. J. 14, 1041–1060.
Reina, A., Jia, X., Ho, J., Nezich, D., Son, H., Bulovic, V., Dresselhaus, M.S., Kong, J., 2009. Nano Lett. 9, 30–35.
Ren, T., Wang, Y., Yu, Q., Li, M., 2019. Mater. Lett. 235, 42–45.
Rengaraj, S., Cruz Izquierdo, Á., Scott, J.L., Di Lorenzo, M., 2018. Sensor. Actuator. B Chem. 265, 50–58.
Saadati, A., Hassanpour, S., de la Guardia, M., Mosafer, J., Hashemzaei, M., Mokhtarzadeh, A., Baradaran, B., 2019. TrAC Trends Anal. Chem. (Reference Ed.) 114, 56–68.
Sadik, O.A., Yan, F., 2007. Anal. Chim. Acta 588, 292–296.
Saeed, A.A., Sánchez, J.L.A., O'Sullivan, C.K., Abbas, M.N., 2017. Bioelectrochemistry 118, 91–99.
Sanni, S.E., Agboola, O., Sadiku, R.E., Emetere, M.E., 2019. Nature of graphene, its chemical structure, composites, synthesis, properties, and applications. In: Handbook of Graphene Set.
Sanvicens, N., Pastells, C., Pascual, N., Marco, M.-P., 2009. TrAC Trends Anal. Chem. (Reference Ed.) 28, 1243–1252.
Sha, J., Li, Y., Villegas Salvatierra, R., Wang, T., Dong, P., Ji, Y., Lee, S.K., Zhang, C., Zhang, J., Smith, R.H., 2017. ACS Nano 11, 6860–6867.
Shahrokhian, S., Ranjbar, S., 2019. ACS Sustain. Chem. Eng. 7, 12760–12769.
Shi, J., Guo, J., Bai, G., Chan, C., Liu, X., Ye, W., Hao, J., Chen, S., Yang, M., 2015. Biosens. Bioelectron. 65, 238–244.
Shirshahi, V., Tabatabaei, S.N., Hatamie, S., Saber, R., 2019. J. Pharmaceut. Biomed. Anal. 164, 104–111.
Singh, C., Ali, M.A., Reddy, V., Singh, D., Kim, C.G., Sumana, G., Malhotra, B., 2018. Sensor. Actuator. B Chem. 255, 2495–2503.
Singh, M., Holzinger, M., Tabrizian, M., Winters, S.a., Berner, N.C., Cosnier, S., Duesberg, G.S., 2015. J. Am. Chem. Soc. 137, 2800–2803.
Siontorou, C.G., Nikoleli, G.P., Nikolelis, D.P., Karapetis, S., Nikolelis, M.T., 2019. Graphene-based biosensors: design, construction, and validation. Toward a nanotechnological tool for the rapid in-field detection of food toxicants and environmental pollutants. In: Handbook of Graphene Set.
Song, S., Wang, L., Li, J., Fan, C., Zhao, J., 2008. TrAC Trends Anal. Chem. (Reference Ed.) 27, 108–117.
Song, Y., Luo, Y., Zhu, C., Li, H., Du, D., Lin, Y., 2016. Biosens. Bioelectron. 76, 195–212.
Song, Z., Wang, X., Zhu, G., Nian, Q., Zhou, H., Yang, D., Qin, C., Tang, R., 2015. Small 11, 1171–1176.
Sreeprasad, T., Berry, V., 2013. Small 9, 341–350.
Stoller, M.D., Park, S., Zhu, Y., An, J., Ruoff, R.S., 2008. Nano Lett. 8, 3498–3502.
Subramanian, P., Barka Bouaifel, F., Bouckaert, J., Yamakawa, N., Boukherroub, R., Szunerits, S., 2014. ACS Appl. Mater. Interfaces 6, 5422–5431.
Sun, T., Xia, N., Liu, L., 2016. Nanomaterials 6, 20.
Swathi, R., Sebastian, K., 2009. J. Chem. Phys. 130, 086101.
Syama, S., Mohanan, P., 2016. Int. J. Biol. Macromol. 86, 546–555.
Teengam, P., Siangproh, W., Tuantranont, A., Henry, C.S., Vilaivan, T., Chailapakul, O., 2017. Anal. Chim. Acta 952, 32–40.
Thakur, B., Zhou, G., Chang, J., Pu, H., Jin, B., Sui, X., Yuan, X., Yang, C.H., Magruder, M., Chen, J., 2018. Biosens. Bioelectron. 110, 16–22.
Tian, J., Luo, Y., Huang, L., Feng, Y., Ju, H., Yu, B.Y., 2016. Biosens. Bioelectron. 80, 519–524.
Tiwari, S.K., Kumar, V., Huczko, A., Oraon, R., Adhikari, A.D., Nayak, G., 2016. Crit. Rev. Solid State Mater. Sci. 41, 257–317.
Tyagi, S., Kramer, F.R., 1996. Nat. Biotechnol. 14, 303–308.
Ulm, H., Wilmes, M., Shai, Y., Sahl, H.G., 2012. Front. Immunol. 3, 249.
Veerapandian, M., Hunter, R., Neethirajan, S., 2016. Talanta 155, 250–257.
Viraka Nellore, B.P., Kanchanapally, R., Pedraza, F., Sinha, S.S., Pramanik, A., Hamme, A.T., Arslan, Z., Sardar, D., Ray, P.C., 2015. ACS Appl. Mater. Interfaces 7, 19210–19218.
Voiry, D., Yang, J., Kupferberg, J., Fullon, R., Lee, C., Jeong, H.Y., Shin, H.S., Chhowalla, M., 2016. Science 353, 1413–1416.
Wang, B., König, M., Bromley, C.J., Yoon, B., Treanor, M.J., Garrido Torres, J.A., Caffio, M., Grillo, F., Früchtl, H., Richardson, N.V., 2017. J. Phys. Chem. C 121, 9413–9423.
Wang, T., Huang, D., Yang, Z., Xu, S., He, G., Li, X., Hu, N., Yin, G., He, D., Zhang, L., 2016. Nano-Micro Lett. 8, 95–119.
Wang, Y., Bai, X., Wen, W., Zhang, X., Wang, S., 2015. ACS Appl. Mater. Interfaces 7, 18872–18879.
Wei, D., Liu, Y., 2010. Adv. Mater. 22, 3225–3241.
Wen, J., Li, W., Li, J., Tao, B., Xu, Y., Li, H., Lu, A., Sun, S., 2016. Sensor. Actuator. B Chem. 227, 655–659.
Wen, L.X., Lv, J.J., Chen, L., Li, S.B., Mou, X.J., Xu, Y., 2019. Microchim. Acta 186, 122.
Wu, G., Dai, Z., Tang, X., Lin, Z., Lo, P.K., Meyyappan, M., Lai, K.W.C., 2017. Adv. Healthc. Mater. 6, 1700736.
Wu, J., Chen, A., Qin, M., Huang, R., Zhang, G., Xue, B., Wei, J., Li, Y., Cao, Y., Wang, W., 2015. Nanoscale 7, 1655–1660.
Wu, Y.M., Cen, Y., Huang, L.J., Yu, R.Q., Chu, X., 2014. Chem. Commun. 50, 4759–4762.
Xia, M.Y., Xie, Y., Yu, C.H., Chen, G.Y., Li, Y.-H., Zhang, T., Peng, Q., 2019. J. Contr. Release 307, 16–31.
Xue, T., Cui, X., Guan, W., Wang, Q., Liu, C., Wang, H., Qi, K., Singh, D.J., Zheng, W., 2014. Biosens. Bioelectron. 58, 374–379.
Yang, J.K., Kwak, S.Y., Jeon, S.J., Lee, E., Ju, J.M., Kim, H.I., Lee, Y.S., Kim, J.H., 2016. Nanoscale 8, 12272–12281.
Yang, X.X., Li, C.M., Li, Y.F., Wang, J., Huang, C.Z., 2017. Nanoscale 9, 16086–16092.
Ye, H., Duan, N., Gu, H., Wang, H., Wang, Z., 2019. Microchim. Acta 186, 173.
Ye, S., Shao, K., Li, Z., Guo, N., Zuo, Y., Li, Q., Lu, Z., Chen, L., He, Q., Han, H., 2015. ACS Appl. Mater. Interfaces 7, 21571–21579.
You, Z., Qiu, Q., Chen, H., Feng, Y., Wang, X., Wang, Y., Ying, Y., 2020. Biosens. Bioelectron. 150, 111896.
Yu, N., Zhang, X., Gao, Y., You, H., Zhang, J., Miao, P., 2019. ACS Omega 4, 14312–14316.
Yuan, K., Mei, Q., Guo, X., Xu, Y., Yang, D., Sánchez, B.J., Sheng, B., Liu, C., Hu, Z., Yu, G., 2018. Chem. Sci. 9, 8781–8795.
Zaid, M.H.M., Abdullah, J., Yusof, N.A., Sulaiman, Y., Wasoh, H., Noh, M.F.M., Issa, R., 2017. Sensor. Actuator. B Chem. 241, 1024–1034.
Zaid, M.H.M., Abdullah, J., Yusof, N.A., Wasoh, H., Sulaiman, Y., Noh, M.F.M., Issa, R., 2020. J. Sens. 2020.
Zaouri, N., Cui, Z., Peinetti, A.S., Lu, Y., Hong, P.Y., 2019. Environ. Sci. Water Res. Technol. 5, 2260–2268.
Zhang, H., Zhang, H., Aldalbahi, A., Zuo, X., Fan, C., Mi, X., 2017c. Biosens. Bioelectron. 89, 96–106.
Zhang, M., Yin, B.C., Wang, X.F., Ye, B.C., 2011. Chem. Commun. 47, 2399–2401.
Zhang, Q., Zhang, D., Lu, Y., Yao, Y., Li, S., Liu, Q., 2015b. Biosens. Bioelectron. 68, 494–499.
Zhang, Q., Zhang, D., Xu, G., Xu, Y., Lu, Y., Li, S., Liu, Q., 2017a. Sensor. Actuator. B Chem. 242, 443–449.
Zhang, Y., Chen, X., Roozbahani, G.M., Guan, X., 2018. Anal. Bioanal. Chem. 410, 6177–6185.
Zhang, Z., Xia, X., Xiang, X., Huang, F., Han, L., 2017b. Sensor. Actuator. B Chem. 249, 8–13.
Zhao, W., Xing, Y., Lin, Y., Gao, Y., Wu, M., Xu, J., 2020. Sens. Actuators Rep. 2, 100004.
Zheng, Q., Wu, H., Shen, Z., Gao, W., Yu, Y., Ma, Y., Guang, W., Guo, Q., Yan, R., Wang, J., 2015. Analyst 140, 6660–6670.
Zhou, C., Zou, H., Li, M., Sun, C., Ren, D., Li, Y., 2018. Biosens. Bioelectron. 117, 347–353.
Zhou, J., Ren, M., Wang, W., Huang, L., Lu, Z., Song, Z., Foda, M.F., Zhao, L., Han, H., 2020. Anal. Chem. https://doi.org/10.1021/acs.analchem.0c00200.
Zhu, C., Du, D., Lin, Y., 2017. Biosens. Bioelectron. 89, 43–55.
Zhu, F., Zhao, G., Dou, W., 2018. Microchim. Acta 185, 455.
Zhu, X., Li, J., He, H., Huang, M., Zhang, X., Wang, S., 2015. Biosens. Bioelectron. 74, 113–133.
Ziółkowski, R., Oszwałdowski, S., Kopyra, K.K., Zacharczuk, K., Zasada, A.A., Malinowska, E., 2020. Microchem. J. 154, 104592.